Results in Engineering 25 (2025) 104120

Contents lists available at ScienceDirect

Results in Engineering

journal homepage: www.sciencedirect.com/journal/results-in-engineering

Case report

Working fluid selection and performance analysis for subcritical organic Rankine cycles

Mohammad Shalby [a,*], Abdullah Marachli [a], Ahmad A Salah [b]

[a] Department of Mechanical Engineering, Faculty of Engineering, Al-Hussein Bin Talal University, Ma'an 71111, Jordan
[b] Department of Electrical Engineering, Faculty of Engineering, Al-Hussein Bin Talal University, Ma'an 71111, Jordan

ARTICLE INFO

Keywords:
Organic Rankine cycle
Low-temperature heat recovery
Working fluids
Power generation
Renewable energy

ABSTRACT

The urgent need to mitigate global warming and the energy crisis has driven the exploration of zero-carbon energy solutions. The organic Rankine cycle (ORC) offers an efficient method to utilize low-grade heat sources while adhering to environmental constraints. This study comprehensively reviews factors influencing working fluid (WF) selection for ORC systems, highlighting their critical role in system performance and design. Additionally, the study evaluates WF performance across various subcritical ORC configurations using environmental and thermo-economic indicators.

Abbreviations and Subscripts
Organic Rankine Cycles ORC_s
Working fluids   WFs
Combined Heat and Power   CHP
Global Warming Potential   GWP
Decamethylcyclopentasiloxane   D5
Decamethyltetrasiloxane   MD2M
Dodecamethylcyclohexasiloxane   D6
Dodecamethylpentasiloxane   MD3M
Hexamethyldisiloxane   MM
Octamethyltrisiloxane   MDM
Ozone Depletion Potential   ODP
Perfluorocarbons   PFCs
Hydrocarbons   HCs
Hydrochlorofluorocarbons   HCFCs
Hydrofluorocarbons   HFCs
Hydrolfluoroolefins   HFOs
Chlorofluorocarbons   CFCs
Mass flow rate (kg s^{-1})   mf
Power or pressure (kPa,MPa)   P,p
Temperature, (°C, K)   T
Work (W)   W
Heat input, (W)   Q
Efficiency (%) η
Effectiveness (%)   Ɛ
Internal heat exchanger   IHE
Enthalpy Drop (Kj/kg).   ΔH
Volume (m^3)   V
Levelized Cost of Electricity   LCOE
Transfer area of total net power output (W/m^2)   APR
Pinch point temperature difference (K) ΔT_{min}
Turbine sizing parameter   SP
Volumetric ratio   VFR
Pressure ratio or turbine inlet pressure to critical pressure   PR or TIP/P_{cr}
High and low-temperature loop   HTL, LHL
Area (m^2)   A
P (kg/m^3)   Density
Minimum electricity production cost   EPC
Internal Combustion Engine   ICE
Waste heat recovery   WHR
Cr   Critical
Con   Condenser
Ev   Evaporator
Ex   Exergy
F   Flow
Hs   Heat source
Max or opt   Maximum
N   Net power
P   Pump
Sup   Superheating
Tot   Total

* Corresponding author.
E-mail address: mohammad.shalby@ahu.edu.jo (M. Shalby).

https://doi.org/10.1016/j.rineng.2025.104120
Received 27 November 2024; Received in revised form 29 December 2024; Accepted 20 January 2025
Available online 27 January 2025

T	Turbine or expander
Th	Thermal
1,2,3	State point

1. Introduction

Power generation from renewable energy sources is at the forefront of the global effort towards providing sustainable, long-term, and environmentally friendly energy sources [1–3]. Various systems have been proposed and implemented to extract power from renewable resources to reduce dependency on traditional fossil fuels and mitigate environmental impacts. These systems include solar photovoltaic (PV), wind turbines, small hydro generators, pumped hydro systems, geothermal plants, biomass energy facilities, and battery energy storage units [4]. These technologies can also be classified as high and low-temperature energy technologies. High-temperature energy technologies often involve more complex and specialized systems, such as concentrated solar power and nuclear reactors operating at excessively high temperatures, which offer the potential for higher energy conversion efficiencies [5]. Conversely, low-temperature technologies (lower than 700–800 °C) capture energy at relatively low-temperature ranges, such as biomass, geothermal, solar, and waste heat of industrial processes [6,7].

Electricity can be generated from photovoltaic cells by converting sunlight into electricity directly or employing concentrated solar power to focus sunlight on fluids that drive turbines. Also, combined heat and power systems, Organic Rankine Cycle Technology (ORCs), or thermoelectric generators to produce electricity or enhance energy efficiency from industrial processes, geothermal, solar, and waste heat [8,9]. Furthermore, combustion, gasification, and anaerobic digestion are used for power extracted from biomass [10]. ORCs are a promising technology for generating power from low, medium, and high-temperature heat quality sources such as biomass, solar thermal, geothermal, waste incinerators, engines or gas turbines, and industrial recovery waste heat. Thermal power can also be produced from high-temperature sources [11]. Recently, these technologies have received special attention due to the energy crisis, high prices of fuels, global warming, and emission regulations. This calls for the use of more environmentally friendly and efficient energy systems in the future [12–14]. ORC has many benefits over other technologies, such as reliability, considerably low costs, safety, flexibility, minimum requirements maintenance, suitable operational parameters, and self-governing operation conditions [15]. Moreover, high efficiency can be ensured in the ORC processes from low, medium temperature heat sources connecting to small-scale applications. It also can produce electricity without burning fossil fuels, which means a lower carbon footprint. ORC technology has a broad field of application [16,17]. and is widely used in industries [17]. In addition, it can be useful as a cooling system in offshore and onshore wind farms. Furthermore, using a thermal tank with an ORC for energy storage makes this system more flexible.

The actual implementations of ORCs started in 1904 with engine capacities of 4.5 kW and 11 kW using Sulfur Dioxide as the working fluid [18]. 1940, D'Amelio designed a geothermal plant using ethylene as the working fluid. Nowadays, commercial ORC plants constructed by leading companies Ormat and Turboden have a capacity of >25 MW. Ormat has built over 3000 units up to 4 kW and >500 units of 1–25 MW[9]. >20 different Working Fluids (WFs) have been used to date, e.g., silicon fluids, hydrocarbons, and old and new-generation refrigerants, depending on the application [19].

A literature review reveals that the effect of cycle and WF parameters on thermo-economic comparisons of different ORC configurations is highly complex [20]. Selecting suitable WFs for an ORC is a challenging task that requires several considerations. Whether it is a pure substance or a mixture, various requirements must be met, considering factors such as the heat source temperature, thermodynamic and heat transfer properties, chemical reactivity of materials, environmental and legislative concerns, and operational costs. In this study, the geometrical configuration of the ORC system is analyzed in detail, highlighting its influence on the interaction between system parameters, cycle performance and WF characteristics. This aspect provides new insights into how specific configurations contribute to system efficiency and sustainability. Meeting these requirements is critical to maximizing system performance, ensuring environmental sustainability, and improving the economic viability of ORC technology. This study will draw a guide to selecting the most appropriate working fluids for various ORC applications by considering the characteristics of different WFs using environmental and thermo-economic indicators.

2. The organic Rankine cycle (ORC)

The working process of ORC is based on a closed-loop thermodynamic cycle like the Rankine Cycle, which typically uses water as the working fluid. Instead of steam, the ORC system used organic fluids with a molecular mass higher than water. These conditions reduce the number of turbine rotations and thus the vapor pressures, which leads to minimizing the erosion of metal parts, especially the blades of the last turbine stages [9]. A simple ORC system is characterized by a specific configuration of processes, including evaporation, isentropic expansion, condensation, and compression. It consists of four components that are responsible for processes: process 1–2 (circulating and pressurizing the working fluid through a pump), process 2–3 (evaporation of the working fluid from an external heat source in the evaporator), process 4–5 (expansion through the turbine/ an expander), and process 5–1 (heat rejection in condenser to cooling media), as shown in Fig. 1. Heat energy through expansion is converted into mechanical and then to electrical in generator The external sources may be any renewable energy system or a heat recovery system (HRS). In some modifications of ORC, a recuperator can be installed as a liquid preheater between the pump outlet and the expander outlet or heat water cylinder to improve cycle performance.

In literature, the organic applications of ORC depend on several factors, including heat source characteristics, choice of the working fluid, system scale, desired power output, environmental considerations, economics, regulations, integration possibilities, heat sink availability, and geographic location [12–14,16,22–24]; the most important one can be summarized as follows:

2.1. Characteristics of heat source

The temperature and type of heat source significantly influence ORC applications, which are often used with low- to medium-temperature heat sources. ORC technology efficiently converts heat into mechanical work for electricity generation or other mechanical processes. Common heat sources include solar, geothermal, biomass, heat recovery systems, industrial processes after fossil fuel burning, municipal solid waste gasifier + syngas, and surface seawater cleaning. ORC systems can utilize diverse eat sources, classified as closed systems, such as solar energy, biomass combustion and industrial chemical reactions or open systems, such as industrial processes, ICE exhaust gases, gas turbine exhaust and geothermal water where the cooled stream is exhausted, to the atmosphere after heat exchange. The temperature of the heat source plays a vital role in the selection of the working fluid (subcritical, transcritical, or supercritical), categorized as a high range of (> 650ºC), a medium range of (230 – 650 ºC), and a low range of (< 230 ºC) [12]. This study focuses on low and medium heat sources (80–380 ºC), where a higher level could be more effective in other applications, such as steam turbines working in the combined cycle [25,26]. The heat source capacity, commonly measured in megawatts (MW) or kilowatts (kW), determines an ORC system's energy output and power potential. The dynamic of heat sources, including variations in temperature, flow rate, and availability, affects whether energy storage is necessary. The cost of ORC components varies based on the system's size, complexity, design,

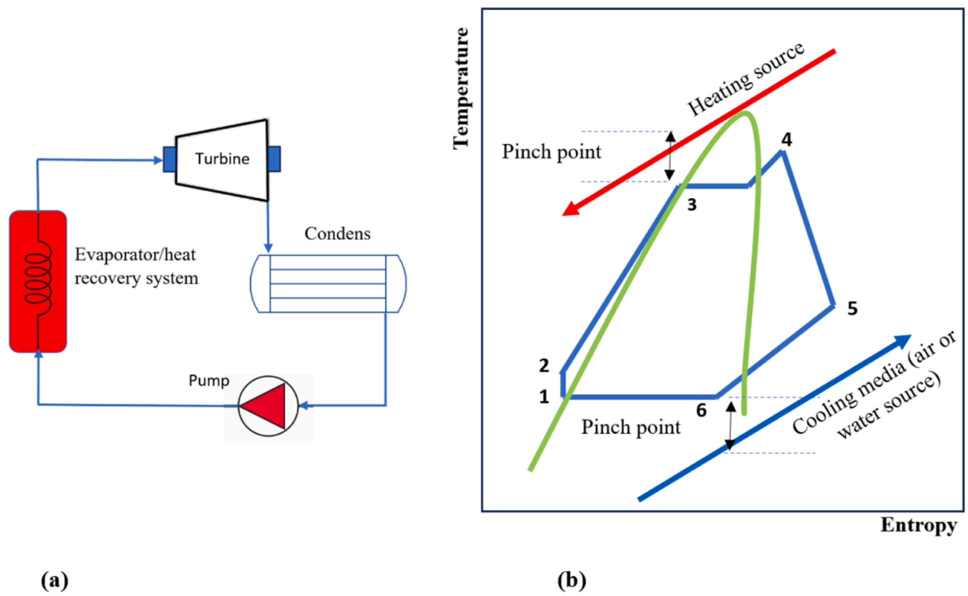

Fig. 1. a) Component of the Organic Rankine Cycle [16]. b) Thermodynamic cycle on T-s diagram [21].

and the selected components. It includes additional parts like auxiliaries' heat exchange devices, solar collector drilling, and exploration operations. These costs will vary depending on the specific application, the scale of the ORC system and technological advancements over time.

2.2. Cycle type

Generally, the ORC is a thermodynamic cycle that converts heat into mechanical work, like the Rankine cycle typically used for steam turbines. The cycle type of the ORC strongly depends on the heat source temperature and the pinch temperature difference $\Delta T_{\min}$, which plays a key role in working fluid selection and then attending to the optimal cycle layout with a higher cycle efficiency. The cycle type can be categorized as follows: 1) finite capacity heat, open source without an outlet temperature limitation $T_{\min}$; 2) finite capacity heat source with outlet temperature limitation, which can be either available type sources, $T_{\min}$ is the outlet temperature limitation or closed type, $T_{\min}$ always has a relatively high temperature with a high cycle efficiency; 3) an infinite heat source with a constant temperature like evaporation or condensation processes. Usually, ηth the ORC varies between 8 and 20 %, with higher values related to the cycle with the highest T_{hs} and internal heat exchanger.

2.3. End use

The choice of the specific ORC system and working fluid depends on the heat source's temperature and the system's end use. As ORC technology is an attractive option for increasing energy efficiency and utilizing low-temperature waste heat, the end-use applications include electricity generation, CHP, desalination, cooling, HAVC, mechanical driving, ice making, etc. Good thermal matching between the heat source and the working fluid is needed to obtain the highest possible power and best efficiency. This could be achieved by appropriately selecting the ORC component, cycle parameters, plant end objective, and ambient conditions.

3. Working fluids classification

Choosing a working fluid is a critical aspect of the ORC as it plays a crucial role in the energy conversion process within the ORC, which directly significantly influences the cycle's efficiency and performance. Thus, classifying working fluids for ORC systems is essential in determining the optimal fluid for a specific application. The ORC working fluids can be classified based on several criteria, such as their thermodynamic properties, environmental impact, safety, and application temperature range. Several works have discussed selecting and categorizing ORC working fluids based on various criteria. Naqvi et al. [27] proposed a method for choosing the optimum working fluid based on thermal efficiency, Global Warming Potential (GWP), Ozone Depletion Potential (ODP), and Atmospheric Lifetime. Krempus et al. [28] analyzed the benefits of using binary mixtures as working fluids in ORC systems, considering efficiency, GWP, and flammability. Herath et al. [29] studied the performance of different working fluids, including R-134a, R-245fa, Benzene, Methanol, Ethanol, Acetone, and Propane, and found that Benzene and Methanol-based ORC systems performed more efficiently. Eyerer et al. [30], Considering material compatibility and system performance, investigated the applicability of modern fluids, such as R1233zd(E) and R1224yd(Z), as drop-in replacements for R245fa in ORC systems. Györke et al. [31] proposed a novel categorization of working fluids to help find the thermodynamically optimal fluid for a given heat source.

Several methodologies are used to classify the working fluids of the ORC, the most important of which are summarized in [12,15,32–34]. The following are the most critical factors that can be utilized to classify ORC working fluid:

3.1. According to the chemical elements or structure included in its composition

The fluids used in ORC systems can be categorized based on their chemical composition and structure. Table 1 summarizes these categories and specific examples for each type.

3.2. According to GWP and ODP levels

According to GWP and ODP levels, the environmental impact of fluids can be classified into three categories [22,35–37]:

1. Fluids with low GWP (<150) and zero for ODP are considered environmentally friendly.
2. Fluids with medium GWP (between 150 −2500) and ODP values below 0.1 fall into a moderate impact category.

Table 1
Classification of ORC Fluids by Chemical Composition and Structure.

ORC Fluid types	Chemical Composition and Structure / Example
1. Hydrocarbons (HCs)	• **Linear Alkanes**: Pentane (R601), Hexane, Heptane, Ethane, Octane, Butane (R600), Propane (R290), Nonane, Decane • **Branched Alkanes:** Isopentane, Isobutane (R600a), Isohexane • **Cyclic Alkanes:** Cyclopentane, Cyclopropane, Cyclohexane • **Aromatics:** Benzene, Toluene
2. Hydrofluorocarbons (HFCs) and Hydrochlorofluoroolefins (HCFOs)	• **HFCs:** R245fa, R125, R134a, R143a, R152a, R365mfc, R407a, R507a, R410a, R404a, R422a, R507, R508a • **HCFOs:** R1234yf, R1234ze
3. Hydrochlorofluorocarbons (HCFCs)	• **Examples:** R123, R21, R22, R124, R141b, R142b, R225ca, R401a, R402a, R403b
4. Chlorofluorocarbons (CFCs)	• **Examples:** R12, R13, R113, R114, R115, R502, R503
5. Perfluorocarbons (PFCs)	• **Examples:** R14, R116 • These are powerful greenhouse gases with high global warming potentials (6500–9200).
6.Siloxanes	• **Linear Siloxanes:** Octamethylcyclotetrasiloxane (D4, D5, D6) • **Cyclic Siloxanes:** Hexamethyldisiloxane (MM), Octamethyltrisiloxane (MDM, MD2 M, MD3 M, MD4 M)
7. Alcohols	• **Examples:** Ethanol, Methanol
8. Ethers	• **Example:** Dimethyl Ether (R170)
9. Hydrofluoroethers (HFE)	• **Examples:** HFE7000, HFE7100, HFE7500
10. Fluid Mixtures	• **Zeotropic Mixtures:** Compositions differ in liquid and vapor phases; do not boil at constant temperatures. • **Examples:** R404a (R125/143a/134a), R407c (R32/125/134a), R417a (R125/R134a/R600) • **Azeotropic Mixtures:** Vapor and liquid phases retain identical compositions. • **Examples:** R-502 (R22 and R115), R-503 (R23 and R13)
11. Inorganic Fluids	• **Examples:** CO2 (R744), NH3, Water, Air

3. Fluids with high GWP (greater than 2500) and ODP values above 0.1 are considered to have a significant environmental impact.

Since 2010, the use of ozone-depleting refrigerants such as R21, R22, R123, and R245fa has been prohibited due to their significant environmental impact. In Europe, regulations are becoming even stricter: until 2025, only refrigerants with a GWP lower than 2500 will be permitted, and by 2030, refrigerants with a GWP greater than 150 will be banned. As a result, common refrigerants like R134a, R125, R404a, R407c, R507a, and R410a—along with R32 in the future—will no longer be allowed. The focus is now shifting towards Hydrofluoroolefins (HFOs), such as R1336mzz, R123yf, R1234ze(Z), and R1233zd(E), all of which have a GWP ($\sim<10$) and show great potential for sustainable use [38]. Additionally, refrigerant mixtures based on HFOs, like R448a, R449a, R450a, and R513a, are increasingly being developed and adopted [17]. Table 2 comprehensively summarizes the physical, safety, and environmental data of the working fluids (WFs) covered in the literature. These data underscore the importance of selecting WFs that align with international protocols, which now mandate zero ODP and low GWP (below 150) while ensuring high thermal efficiency in ORC systems. Given these criteria, the only viable alternatives are low-GWP HFCs, mixture WFs, and natural refrigerants such as carbon dioxide, ammonia, hydrocarbons (e.g., propane, butane, pentane, and cyclohexane), and water. Additionally, hydrofluorochemicals like HFOs and hydrochlorofluoroolefins (HCFOs) present promising options [39,40]. To replace high-GWP and ODP working fluids, hydrocarbons like propane (R290), butane (R600), pentane (R601), and cyclohexane are being widely used in ORC systems, either as pure substances or in hydrocarbon blends containing ethane (R170). Using these mixtures provides an opportunity to optimize both the flammability and GWP levels of WFs during production [38]. Moreover, zeotropic mixtures are exciting because they reduce thermodynamic irreversibility, especially in condensers. When using these mixtures, the effective temperature glide in both the condenser and evaporator can significantly enhance both first- and second-law efficiencies in many cases. This dual benefit of improved efficiency and controlled environmental impact positions zeotropic mixtures as a crucial component in the future of ORC systems [41].

3.3. According to safety and dangerousness

The ASHRAE 34 safety classification standard divides working fluids into categories based on flammability and toxicity during handling and operation. These categories help ensure the safe use of fluids in ORC systems and other applications.

- **Flammability Classification:**
  - **Class 1:** Fluids that do not propagate a flame in open air under normal conditions.
  - **Class 2:** Fluids that may propagate a flame in open air under specific conditions.
  - **Class 3:** Fluids with high flammability.
- **Toxicity Classification:**
  - **Class A:** Fluids with no evidence of toxicity at concentrations below 400 ppm.
  - **Class B:** Fluids with evidence of toxicity at concentrations below 400 ppm.

Combining these classifications creates a fluid safety index, which includes the following categories:

- **A1:** Non-flammable and non-toxic.
- **A2:** Lower flammability and non-toxic.
- **A3:** Non-toxic but flammable.
- **B1:** Non-flammable but toxic.
- **B2:** Toxic with lower flammability.
- **B3:** Toxic and flammable.

Recently, two additional safety classes-A2 L and B2 L were introduced to address mildly flammable fluids, enhancing the classification system [42,43].

Table 3 summarizes the toxicity and flammability characteristics of various working fluids. The goal is to select fluids that balance safety with environmental considerations. Ideally, the working fluid should have low toxicity to ensure safe maintenance and operation, minimizing hazardous conditions for employees. Fluids with the smallest potential for GWP and ODP, such as hydrocarbons (HCs), siloxanes, Hydrofluoroolefins (HFOs), and specific refrigerants like R152, R41, R161, R21, R123, methanol, and ethanol, are preferred. Safety considerations also favor fluids with minimal toxicity and flammability, including R22, R41, R124, R134a, R236ea, R718 (H_2O), R744 (CO_2), and R729. As highlighted in Tables 2 and 3, no single working fluid perfectly meets all these criteria simultaneously. Therefore, selecting the most appropriate fluid requires careful consideration of both safety and environmental impacts.

3.4. Classification of working fluids for ORCs based on vapor curve slope

Working fluids for Organic Rankine Cycles (ORCs) can be classified according to the slope of their saturated vapor curves on a temperature-entropy (T-s) diagram, represented by the parameter $\xi = ds/dT_s$ [44,45], where:

Table 2
Physical, safety and environmental data of the working fluids [15,22,27].

No	Substance	Physical data				Environmental and safety data				Expansion Molecular complexity
		Molecular Mass (kg/kmol)	Tbp (°C)	Tcr (°C)	Pcr (MPa)	Atmospheric lifetime (years)	ODP	GWP (100 yr)	Safety	
Siloxanes										
1	MM hexamethyldisiloxane, ($C_6H_{18}OSi_2$)	162.38	100.25	245.6	1.93	n.a	0	Very low	n.a	dry
2	D5 ($C_{10}H_{30}O_5Si_5$)	370.8	210	346.1	1.15	n.a	n.a	n.a	A3	dry
3	D4 ($C_8H_{24}O_4Si_4$)	*296.6*	175	313.3	1.34	n.a	n.a	n.a	A3	dry
4	MDM ($C_8H_{24}O_2Si_3$)	*236.6*	154	290.9	1.41	n.a	n.a	n.a	n.a	dry
5	MD2 M ($C_{10}H_{30}Si_4O_3$)	310.7	194.4	326.3	1.19	n.a	n.a	n.a	n.a	dry
Hydrofluoroolefins (HFO$_s$)										
1	R1234yf	114.04	−30	94.75	3.36	n.a	0	4	A2L	dry
2	R1234ze(Z)	114	9.721	150.1	3.531	18 days	0	6	A2L	wet
3	R1224yd(Z)	148.5	14.61	155.5	3.337	20days	0.88	0.00023	A1	wet
4	R1233zd(E)	130.5	18.32	166.6	3.531	40.4	0	1	A1	Isen
5	R1336mzz(E)	164	7.5	137.7	3.15	22 days	0	18	A1	Isen
6	R1336mzz(Z) DR-2,	164.05	33.4	171.1	2.9	22 days	0	8.9	A1	dry
Hydrofluorcarbos (HFC$_s$)										
1	R152a	66.05	−24	113.3	4.52	1.4	0	140	A2	wet
2	R41 CH_3F	34.03	−78.1	44	5.9	n.a	0	97	A2	wet
3	R161(C_2H_5F)	48.06	−37.75	102	5.090	0.18	0	12	n.a	wet
4	R134a($C_2H_2F_4$)	102.03	−26.1	101	4.059	13	0	1300	A1	wet
5	R32	52.02	−51.7	78.11	5.784	4.9	0	675	A2L	wet
6	R407C(zeotropic)	86.2	−43.6	86.79	4.597	n.a	0	1800	A1	dry
7	R245fa	134.045	15.04	154.1	4.517	7.6	0	1050	B1	dry
8	245ca($C_3H_3F_5$)	134.04	25.13	174.42	3.925	n.a	0	693	n.a	dry
9	R417a	109	−39.1	87.1	4.036	n.a	0	1950	A1	isent
10	R236ea($C_3H_2F_6$)	152	3.7	139.29	3.5	n.a	0	858	n.a	dry
11	R227ea(C_3HF_7)	170	−18	102	1.92	n.a	0	3220	A1	dry
12	R143a	84.04	−47.22	72.71	3.76	n.a	0	4470	A2	wet
13	R236fa	152	−1.492	124.9	3.2	240	0	8060	A1	dry
14	R365mfc ($C_4H_5F_5$)	148.1	40.2	186.9	3.26	n.a	0	796	A2	dry
15	R507A azeotropic	98.9	−46.7	70.9	37.8	0	0	3985	AEL	dry
Hydrofluoroethers (HFEs)										
1	HFE7100($C_4F_9OCH_3$) methoxy-nonafluorobutane	250	61	195.3	2.24	4.1	0	410	A1	dry
2	HFE7000	200.10	34.17	164.6	2.478	4.9	0	530	A1	dry
Clorofluorcarbos(CFC$_s$) and Perfluorcarbos(PFC$_s$)										
1	R502 (CFC)	111.63	−45.6	82	4.075	Na	0.28	6200		
2	RC318 C_4F_8(PFC)	200	−5.56	116	2.78	n.a	0	10,300	A1	isen
3	R114(CFC)	170.92	3.6	145.7	2.2	300	1	10,040	A1	isen
Hydrochlorofluorocarbons (HCFCs)										
1	R21 ($CHCl_2F$)	102.923	8.9	178.33	5.18	n.a	0.04	151	B1	wet
2	R123	152.93	27.8	183.7	3.668	1.3	0.02	77	B1	dry
3	R141b	116.95	32	204.2	4.249	9.3	0.12	725	A2	isent
4	R22	86.47	−40.9	95.95	4.99	11.9	0.04	1790	A1	Wet
5	R124	136.48	−11.15	122.15	3.062	5.9	0.02	619	A1	isent
6	R142b	100.5	−10	137	4.05	n.a	0.12	2310	A2	Isentrop
Others (Ethers and Alcohols)										
1	Dimethylether R170 (C_2H_6)	46.07	−24.95	126.85	5.34	0.015	0	1	A3	wet
2	Ethanol (C_2H_5OH)	46.07	78.4	240.8	6.148	n.a	0	Low	n.a	wet
3	Methanol (CH_3OH)	32.04	64.4	240.2	8.104	n.a	0	Low	n.a	wet
4	R718 (water)	18	100	374	22.064	n.a	0	<1	A1	wet
5	R744 (CO_2)	44	−87	31	7.38	n.a	0	1	A1	wet
6	R717(ammonia)	17.03	−33.3	132.3	11.33	0.01	0	<1	B2L	wet
Hydrocarbons (HCs)										
1	R600a(isobutane)	58.12	−11.7	135	3.647	0.019	0	3	A3	dry
2	R600(butane)	58.12	−0.5	152	3.796	0.018	0	3	A3	dry
3	R601(pentane)	72.15	36.1	196.5	3.364	0.01	0	5	A3	dry
4	Cyclohexane (C_6H_{12})	84.16	80.7	280.5	4.075	n.a	0	low	A3	dry
5	Butene(C_4H_8)	56.11	−6.46	146	4.005	n.a	0	low	n.a	dry
6	R290(propane)	44.1	−42.1	96.68	4.247	0.041	0	4	A3	wet
7	Isobutene C_4H_8	56.1	−7.1	144.95	4.01	n.a	n.a	n.a	n.a	isen
8	R170 Ethane (C_2H_6)	30.069	−88.58	32	4.87	n.a	0	6	A3	dry
9	Benzene (C_6H_6)	78.112	80.07	289	4.89	n.a	0	low	B2	dry
10	Toluene (C_7H_8)	92.138	110.6	318.6	4.13	n.a	0	low	A3	isent
11	Propylene1270 (C_3H_6)	42.08	−47.8	91.7	4.62	0.001	0	2	A3	wet
12	R601b	72.15	9.5	160.6	3.2	n.a	0	20	A3	dry
13	R601a	72.15	27.8	187.2	3.38	0.009	0	20	A3	dry
14	RC270(cyclopropane)	42.08	−31.5	125.2	5.58	0.44	0	20	A3	wet
15	Cyclopentane (C_5H_{10})	70.13	49.4	238.6	4.51	0.007	0	11	A3	dry
16	Acetone (C_3H_6O)	58	56.07	234.95	4.6	n.a	0	0.5	n.a	wet

Table 3
Toxicity and Flammability of WFs.

		Flammability		
		1 (none)	2 (low)	3 (high)
Toxicity	**A (Low)**	R13, R14, R22, R23, R41, R113, R114, R115, R116, R124, R125, R134a, R227ea, R236ea, R236fa, R417a, R422a, R422d, R423a, RC318, R718 (H_2O), R744 (CO_2), R729 (Air)	R32, R141b, R142b, R143a, R152a, R245ca	R170 (Ethane), R290 (Propane), R600 (Butane), R600a, R601 (Pentane), R601a, Cyclohexane, Toluene
	B (High)	R21, R123, R245fa	Benzene, R717 (Ammonia)	None

1. **Dry Fluids ($\xi > 0$)**: These fluids have a positive slope and are typically characterized by high molecular weight and complex molecular structures. Dry fluids do not condense during expansion, eliminating the risk of turbine blade erosion.
2. **Isentropic Fluids ($\xi = 0$):** These fluids have a vertical slope on the T-s diagram and do not change entropy during the **phase** change. They also do not pose a condensation risk during expansion.
3. **Wet Fluids ($\xi < 0$):** These fluids have a negative slope and are generally low molecular weight with simpler molecular **structures**. Wet fluids tend to condense during expansion, which requires superheating at the turbine intake to prevent condensation, reducing the risk of turbine blade erosion and wear.

Fig. 2. illustrates the importance of superheating wet fluids to ensure safe turbine operation. Other less commonly used classifications in scientific literature focus on the physical properties of fluids, such as critical pressure, boiling point, and molecular weight. Regarding thermal stability, most organic compounds used in ORCs are stable within a temperature range of 250 °C to 400 °C [37–39]

4. General working fluids requirement

High specific heat and density in fluids enhance heat capacity and mass flow rates, improving heat transfer and reducing pump work, which can lower costs. Fluids with low density, while increasing volume flow rates and pressure drops, may require more significant components and higher system costs. Organic fluids with lower specific vapor volumes are cost-effectively preferred, allowing for smaller system components and reduced costs. For small-scale applications, fluids operating at super-atmospheric pressures are more cost-efficient compared to those at sub-atmospheric pressures, which require additional equipment and can increase overall system costs.

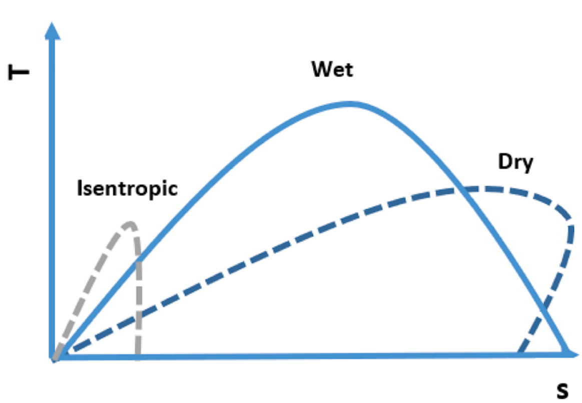

Fig. 2. Types of organic working fluids according to the slope of their saturated vapor curves on T-s diagrams [46].

The selection of an appropriate working fluid is crucial for optimizing the performance, safety, and environmental impact of ORCs. A well-chosen fluid can significantly enhance cycle efficiency, reduce operational costs, and ensure compliance with environmental regulations. Based on existing research, the essential criteria for selecting a working fluid include the following [8,12,38,42,43,47–54]:

1. **Thermodynamic Performance**: High efficiency and specific cycle work, influenced by properties like critical point, specific heat, and density. Fluids with dry or isentropic vapor curves are preferred to avoid turbine damage, and superheating is needed for wet fluids.
2. **Environmental Impact:** Fluids should have zero ODP, low GWP, and short atmospheric lifetimes to comply with environmental regulations.
3. **Safety:** Fluids must be low in flammability, non-toxic, non-explosive, and easy to handle.
4. **Operating Conditions:** Fluids should exhibit acceptable evaporating and condensing pressures (above 0.1 MPa for condensers, below 3 MPa for evaporators), low viscosity for reduced friction losses, and good thermal conductivity for efficient heat transfer. They should also have moderate critical pressures and temperatures, with a critical temperature slightly higher than the expander's inlet temperature.
5. **Chemical Stability:** Fluids should be thermally stable, withstanding temperatures up to 350 °C, to prevent deterioration and decomposition.
6. **Availability and Cost:** Fluids should be easily accessible, cost-effective, and possess low specific volumes for efficient utilization and commercialization.
7. **Latent Heat and Density:** High latent heat and density enable the fluid to absorb more energy from the evaporator, especially when dealing with low-temperature sources.
8. **Lubricant Compatibility:** Fluids must be soluble with lubricant oils used in the system.
9. Freezing Point: The fluid's melting point should be low enough to prevent freezing during operation in cold environments.
10. **Molecular Weight:** Fluids with a higher molecular weight reduce the flow rate and system size, improving turbine efficiency.
11. **Boiling Temperature:** Suitable fluids should have an appropriate boiling point under operating pressures, enabling thermal energy recovery from low-grade heat sources.

According to those mentioned above, a suitable fluid should possess properties such as low specific volumes, high efficiency, moderate pressures in the heat exchangers, low cost, low toxicity, low ODP and low GWP.

5. Analysis literature review

This section provides an in-depth analysis of the literature on selecting WFs and their impact on ORC performance parameters. The characteristics of working fluids, including thermodynamic properties, efficiency, environmental impact, and economic considerations, play a pivotal role in optimizing ORC systems. Understanding how various fluid parameters influence ORC performance under different operational conditions is essential for identifying the most suitable fluids for specific applications.

The reviewed studies examine various WFs under different cycle configurations and temperature conditions, including hydrocarbons, siloxanes, fluorocarbons, and binary mixtures. This literature review summarizes the key findings and highlights critical trends in the selection criteria for WFs and their impact on ORC efficiency, energy, power output, and operational stability. These insights are further supplemented by a comprehensive comparison of studies, as detailed in Table 4, to understand better how WF parameters influence ORC performance in diverse scenarios. The table highlights how these factors influence system efficiency, energy conversion rates, and operational performance by analyzing key attributes such as thermal conductivity, specific heat, viscosity, and molecular weight. Ultimately, this analysis aims to facilitate the selection of optimal working fluids based on application requirements and operational conditions, thereby enhancing the effectiveness of ORC technologies in harnessing waste heat and improving energy recovery.

Tchanche et al. [12] assessed 20 potential working fluids and found that increasing the turbine inlet temperature (T_{int}) leads to a higher turbine outlet volume flow rate (V_5) and improves both thermal efficiency (η_{th}) and exergy efficiency (η_{ex}). They noted that fluids with lower volume flow rates are economically preferable, as this increases turbine inlet pressure and reduces system irreversibility. Optimal condenser temperatures were 5–15 °C above ambient temperature. Laouid et al., [80] examined six working fluids: Cyclopropane, Dimethyl ether, Propyne, R236ea, R-600a and R152a, and observed that η_{ex} initially increases and then decreases at higher evaporation pressures P_{ev} for dry and isentropic fluids (R600a, R236ea). In contrast, it continually increases with P_{ev} for wet fluids (propyne, R152a). Additionally, the net power P_n reaches an optimal value when increasing P_{ev}, with R236ea producing the highest power output, followed by R152a and Cyclopropane having the lowest. The η_{ex} rises with the degree of superheat for all working fluids, with wet fluids showing a slightly greater increase than dry and isentropic fluids. Wet fluids also exhibited a slight increase in P_n. Both η_{ex} and P_n decrease with the increasing PR for all WF types. Furthermore, using an internal heat exchanger IHE and reheating improved η_{ex} but decreased P_n for all WFs and R236ea and propyne were found to be the most effective WF for the ORC systems, both with and without IHE.

The choice of Rankine cycle applications and working fluids classes primarily depends on the heat source's temperature, which determines the maximum achievable temperature, pressure, the size of ORC components and overall performance. Vélez et al. [17] proposed using refrigerants (fluorocarbons) for heat sources temperatures below 175 °C, hydrocarbons for the range 175–250 °C, and siloxanes with a high critical temperature for T_{hs} up to 400 °C. These findings align with Uusitalo et al. [15] and Fernández et al. [81], who investigated various siloxanes for high-temperature ORC applications. They recommended that simple linear siloxanes like MM (hexamethyldisiloxane) and MDM (octamethyltrisiloxane) are stable and more efficient. While more complex siloxanes such as D5 (decamethylcyclopentasiloxane), D6 (dodecamethylcyclohexasiloxane), and MD2 M (decamethyltetrasiloxane) are more suitable for applications requiring lower condensing pressure.

Liu, Chao et al., [56] studied Hexane, Isohexane, R601, R123, and R234fa, showing higher efficiencies for ORC with IHE configuration. Among these, R123 exhibited the most favorable performance, with higher P_n and the η_{th} of ORC being 14.2 % and 13.28 % with and without IHE, respectively. Similarly, Altun et al., [11] investigated real ORC (AFJET geothermal power plant) using R134a and found that when the condenser temperature varies from 18 to 30 °C, the η_{th} decreases from 11.24 % to 9.11 %, and the η_{ex} decreases from 49.37 % to 40.03 %. P_n was also observed to be higher during the winter daytime. Additionally, a performance comparison for a binary geothermal system using η_{th}, recovery efficiency, heat exchanger area per unit power output (APR) and the levelized energy cost (LEC) as indicators was conducted by [70] for subcritical ORC and transcritical power cycles in low temperatures (i.e., 80–100 °C). The results showed that R125 and R123 were the best WF for transcritical and subcritical cycles, respectively.

A related study on subcritical and transcritical cycles for small-scale biomass applications [82] analyzed saturated and superheated (transcritical for decane only) conditions at the turbine inlet. High T_{ev} (200–300 °C) improved η_{th} and P_n for all fluids (toluene, cyclohexane, and decane), with the highest efficiency being achieved for the simple saturated cycle using toluene, followed by the transcritical cycle with decane, and then the superheated cycle with cyclohexane. Including an IHE showed the best efficiency for the transcritical cycle with decane, followed by the simple saturated cycle with toluene and the superheated cycle with cyclohexane.

Quoilin et al., [83] described expansion machines for various working fluids in ORC technology, mapping turbine inlet T_{con} and T_{ev} combinations. The scroll technology was found to allow the lowest P_n (a few hundred watts), while the radial inflow turbine provided the highest power output. Radial inflow turbines showed very low minimum power (between 3 and 4 kW) in applications with low-density fluids at the turbine exhaust. The analysis revealed that high-temperature differences e.g., 250/40 °C) cannot be achieved with volumetric expanders but require multi-stage turbines. Specific working fluids were recommended for different applications: R134a for the geothermal cycle, R245fa for the low-temperature solar application, R123 for the low-temperature WHR cycle, Toluene for the high-temperature WHR cycle and OMTS for the high-temperature CHP cycle.

The possibility of utilizing isentropic binary mixtures composed of a wet and a dry component in ORC systems was studied by [84]. Performance was evaluated in a simple saturated ORC model for T_{hs} between 75 °C and 175 °C, with a fixed sink temperature of 17 °C. Binary mixtures offered better η_{ex} than dry single-component fluids without superheating or regeneration, with significant gains in P_{net} for isentropic mixtures observed, especially for HFC and HC fluids at low temperatures. The increases in P_{net} for isentropic single-component fluids were more pronounced at lower heat source temperatures, with up to 35 % and 15 % gains observed for HFC and HC, respectively, at a source temperature of 77 °C.

In a high-temperature heat source application, T_{hs}, Tauveron and Barbier [85] studied a closed gas turbine cycle combined with ORC using R245fa, R125 and Carbon dioxide. From a thermodynamic perspective, the best solution was using the R125 cycle at supercritical pressure on the precooler's secondary side and subcritical pressure on the intercooler's secondary side, yielding a supplementary power output exceeding 15 MWe and a combined cycle net efficiency of 39 %. Biswas et al., [86] evaluated P_n and η_{th} of simple ORC using R245fa, R11, R113, n-pentane, isopentane, R123 and R1233zd (E). They concluded that the P_n and η_{th} increased for all WFs, keeping P_{ev} from 0.1 MPa to 0.6 MPa, with the highest η_{th} achieved for isopentane and R1233zd (E). It was also noted that each WF has a P_{ev} value that maximizes P_n and η_{th}, with isopentane, n-pentane, and R11 having shorter Pev ranges (up to 0.35 MPa).

Finally, White et al., [87] investigated the effect of the volumetric expansion ratio (VFR= V5/V4 or ρ4=ρ5) on turbine efficiency for seven working fluids, showing that VFR significantly impacts turbine efficiency at different size parameters. For the T_{hs} of 200 °C, a single-stage system with a turbine achieved the highest power output, while for higher T_{hs} (up to 300 °C), cascaded cycles generated up to 6 % more power than single-stage systems due to lower VFR within each cycle. The studied working fluids included isopentane, R245fa, R1233zd, isopentane, n-pentane, cyclopentane, and benzene.

6. Factors affecting the performance of ORC

This section analyzes the effect of critical parameters such as heat source temperatures (T_{hs}), working fluid evaporation temperatures (T_{ev}), pressures at the evaporator inlet (P_{ev}), condenser pressure (P_{con}), ambient conditions, heat exchanger effectiveness (ε), and pinch point temperature difference (ΔT_{min}) on the performance of a subcritical ORC cycle. The thermodynamic performance (net power output P_n, thermal efficiency η_{th}, second law efficiency η_{ex}) and economic performance (turbine sizing parameter SP or volumetric ratio VFR, and heat transfer area APR) are considered. According to Mikielewicz et al., [88],

Table 4
Summary of Working Fluid (WF) Parameters and Their Effects on ORC System Performance.

No	Reference	Type of WFs	T_{hs} (°C)	Heat resource	Objective of study	Cycle type and significant parameters	Main results	Notes
1	Tchanche et al. [22]	(20)[a], R152a,141b,123, R32 R600a, R600,R601, R290,R113,R114 and 134a	90^0C	solar	η_{th}, η_{ex}, V_5, m, PR, ODP and GWP	Simple cycle with preheater and heat storage tank. Micro-turbine. η_t= 0.70 η_p =0.80, T_{ev}=70^0C	There is an optimal value of, $\eta_{th.}$ η_{ex}, for each fluids depending on PR. WFs with lower V are economically preferable	Increasing (Tint) the V_5 increased. R152a, R600, R600a and R290 are most suitable
2	He C et al. [55]	(22)[a] R717, methanol, ethanol,R600, R600a, R114,R245fa,R123, R113,R601a,R141b, toluene,nheptane, cyclohexane, n-nonane, n-decane and n-dodecane.	150^0C	WHR	Pn, working pressure, total heat transfer capacity and expander SP	Simple ORC, η_t= 0.80, η_p =0.75 $\Delta T_{min})_{ev}$=$\Delta T_{min})_{con}$=5^0C	The greater P_{in} will be produced when the T_{cr} of WF_s is slightly (10–40 °C) lower than the inlet T_{hs}., The max value of SP was for n-nonane, n-decane and n-dodecane.	The maximum Pn, suitable working pressure, total heat transfer capacity and expander SP of ORC, R114, R245fa, R123, R601a, n-pentane, R141b, and R113 are suited as WFs in subcritical ORC
3	Liu, Chao et al. [56]	(28)[a] R143a,R32,R22,R290, R134a,R227ea,R152a, RC318,R124,R236fa, R717,R600a,R142b, R114,R600,R245fa, R123,R601,R601a, n-Hexane, Toluene, Propylene, Methanol, Ethanol	85–150 °C	WHR	η_{ex}, optimal evaporation temperature (OET)	Simple cycle without superheating $\Delta T_{min})_{ev}$ 5–20,$\Delta T_{min})_{con}$=5 °C . η_t= 0.80, η_p =0.75	All WFs have optimum(ηex) with increasing Tev except R12, R152a, R124 and R236fa, has no optimal values. T_{hs} should be 18 ± 5° higher than the critical temperature T_{cr},	The maximum η_{ex} will decrease with the increase $\Delta T_{min})_{ev}$.(η_{ex}) max for R236fa=44.54 %. Increasing T_{ev} the ΔH drop in the expander increases, but the mf decreased
4	Iacopo Vaja et al. [57]	(3)[a] Benzene(dry), R11(ies) and R134a (wet)	Up to 470^0C	Internal combustion engine with gas fuel	η_{th}, P_n, working pressure. Flow rate at the expander inlet V4 and the turbine outlet/ inlet volume flow ratio VFR	Simple cycle as bottoming. Tcon = 308 K; η_t= 0.70, η_p =0.8	A maximum η_{th} value of 0.2146 is achieved with benzene at a pressure of 0.44 MPa. which returns a net power output of 376 kW.The max of $\eta_{th,}$ Pn achieved near the Pcr for all WFs.	Vaporizing pressure varying between P_{con} and Pcr;.The best WF is benzene
5	Zhai et al. [48]	(25[a])HC (hydrocarbon) propyne,bentene, butane,tuluene, cyclopentan butene e and(12)[a] HFC,R161, R1234ze(z)R1234yf, R152a (hydro fluorine carbon)	110 °C,130 °C,150 °C	Geothermal	optimizing the Tev to maximize the work output per 1 kg of geothermal water for each working fluid.	Simple cycle without reheating or preheating Pinch evaporator 20 °C Condenser temperature 10,20,30 °C η_t= 0.80, η_p =1 $\Delta T_{min})_{ev}$ 20^0C	Maximal Pn =46.4 kJ/kg $\eta_{th,}$about 10 % for toluene .it higher than for R245fa working fluids were around 62^0C for a 110^0C Ths . 72 ^{0}Cfor a 130^0C T_{hs} and 82^0C for T_hs =150^0C . η_{th} decrease as T_{con} increased.	Best Pn for R1234yf at T_{hs}=150^0C Fluids with double-bond structures, showed higher efficiencies than single-bond fluids
6	Igbong, et al. [58]	(15)[a] R134a,R227ea,R1234zf, R152a,R236fa, R600R236ea,R1234ze (z),R245fa,R1224yd(Z) 7HFE7000,R1233zd(E), R365mfc,R601a	200 °C T_{cr}>150 °C for all WFs	Gas turbine	η_{th}, η_{ex}, VFR V_2,Pn,m_f , heat transfer capacity (UA) $_{evap}$	Simple and recuperated ORC. subcritical, superheated and supercritical conditions. ΔTsup=10^0C, $\Delta T_{min})_{con}$=5 mf = 80 kg s^{-1}. η_t= 0.85, η_p = 0.85 $\Delta T_{min})_{ev}$ 10^0C	The values of SP and VFR increase with a fluid having a high T_{cr}.The evaporators are the main source of exergy destruction in the system	R600, R236fa, R600a R1233dz (E) are suitable for simple subcritical, superheated. For subcritical and superheated with preheating R236fa R236ea.
7	Douvartzides et al. [59]	(42)[a]D6,MD3 M, D5, MD2 M, MM,Decane,o-Xylene,mXylene, Nonane,pXylene, Ethylbenzene,Toluene, Heptane,Benzene,	300^0C	Biomass-boiler	Effect of P_{con},P_{ev} on Pn, η_{th}, η_{ex}, η_{CHP}, V_2	Simple with and without regeneration η_t= 0.80, η_p = 0.80 $\Delta T_{min})_{ev}$ =$\Delta T_{min})_{con}$ 10 °C ε = 0.8.	η_{th}, η_{ex}, increased with increasing P_{ev} for all WFs while with increasing Pev, the Pn increases	For maximum Pn and η_{th} R113, R141b, R245fa Cyclohexane, Cyclopentane, Benzene and

(continued on next page)

Table 4 (*continued*)

No	Reference	Type of WFs	T_{hs} (°C)	Heat resource	Objective of study	Cycle type and significant parameters	Main results	Notes
		Cyclohexane,Hexane, Cyclopentane,R113, R365mfc,Pentane, R141b,Isopentane,R123, R11,R245ca,R1233zd (E), R245fa, Neopentane,R1234ze (Z), R114,R236ea,R236fa, RC318,R142b,R124, R227ea,R1234ze(E), R1234yf				P_{con}=10–500kPa P_{ev} up to 3.5 MPa	proportionally for refrigerants and siloxanes, while it increases and then decreases for hydrocarbons	Toluene. The main exergy destruction in the plant takes place in the evaporator and the condense
8	Feng et al. [60]	R123	150^{0}C	WHR	Effect of Pev, Tev, ΔTmin and Degree of superheat ΔTsup on η_{th}, η_{ex}, Pn and the ratio of the total heat transfer area of total net power output APR(W/m^2) using Sensitivity analysis	Simple with and without regeneration. Fixed T_{hs}. ηt= 0.80, ηp = 0.80 ΔTmin)ev = 10 °C, ΔTmin)con=5 °C, ΔTsup=10 °C	Increase of Pev and Tev, the η_{th}, η_{ex} increased. Keep rising with P_{ev} the APR decreases at first and then increases, while the Pn presents the opposite trend. With the increase of $\Delta T_{min})_{ev}$, the Pn and η_{ex} decrease, while the APR increases.	An increase in the T_{con} leads to a decrease in the η_{th}, η_{ex} and Pn and an increase in the APR values. that with the increase of ΔT_{sup}, the Pn decreases, while the η_{th} and APR increase.
9	Bahrami et al. [61]	(9)[a]FC72, FC87, HFE7100, HFE7000, Novec649, n-pentane, n-decane, R245fa, and toluene.	80 °C and 140 °C	combined cycle Stirling-ORC	Thermodynamic investigation and environmental consideration	Simple ORC as bottoming with Stirling engine. ηt= 0.90, ηp = 0.50 ΔTmin) con = 5 °C, ε=0.9.	η_{Tot} increased by 4 % to 8 % up to 42 %. compared to standard cycle for all WFs. The best are toluene, HFE7100, and n-pentane.	n-decane shows the best $\eta_{th.}$ For practical purpose the toluene is the best candidates.
10	Zhang et al. [62]	(11)[a]R600,R601b,R601, R601a,R600a,R1234fy, R161,R245fa, R152a, RC270, Cyclopentane	100–200 °C	WHR	Effect of HX type on thermo-economic parameters. minimum electricity production cost (EPC)	Simple ORC ΔTmin)con =$\Delta Tmin)_{ev}$ =8 °C	EPC, Pn and total cost also increases if *Pev* increases for T_{hs} higher than 82 °C .The best HE is finned tube bundles with circular fins as evaporator and a shell-and-tube HX as condenser (ORC-FS)	RC270, R600a, R600, R601b, R601a and R601 are recommended.
11	Tao Zhang et al. [63]	(42)[a] R218,R143a, R32, R134a, R152a, R124, R236ea propylene, R22, RC318, propane, R227ea, R142b perfluorobutane, nonane Trifluoroiodomethane, dimethylether, Isobutane, butene, *trans*-butene *cis*-butene, benzene,R245fa, R245ca, decane, dodecane, butane, neopentane,R123, R365mfc, isopentane, pentane, isohexane, hexane, heptane, cyclohexane, toluene, octane, ammonia, perfluoropentane, water	250 °C 300 350 - 400 450 –500 ^{0}C	WHR	The relationship between T_{hs}, working fluid physical properties, and system net output	Simple ORC with super heating ηt= 0.80, ηp = 0.80 ΔH_{sup}= 5 ^{0} °C $\Delta Tmin)_{con}$ =ΔTmin)ev =15 °C	Parabola variation relationship between T_{cr} and Pn. Using working fluid with a high temperature ratio can always improve Pn	Relationship between system Pn and working fluid Tcr, system T_{ev}/P_{ev}, and T_{con}/P_{con} by different heat source temperatures
12	Astolfi et al. [64]	(54)[a] 12 Alkanes Propane, Isobutane, Butane, Neopentane, Isopentane, Pentane, Isohexane, Hexane, Heptane, Octane,	120–180 ^{0}C	Geothermal	the selection of the optimal combination of working fluid and cycle configuration	Simple with /without regeneration. Superheated and saturated η_t= 0.85, η_p = 0.70 ΔH_{sup}= 5 ^{0} °C	Optimal plant efficiencies are obtained for fluids with a Tcrit/ Ths parameter between 0.88 and	When subcritical cycles are considered, superheating is not profitable and optimal cycles

(continued on next page)

Table 4 (*continued*)

No	Reference	Type of WFs	T_{hs} (°C)	Heat resource	Objective of study	Cycle type and significant parameters	Main results	Notes
		Nonane, Decane 16 Other hydrocarbons Cyclopropane, Cyclopentane, Cyclohexane, Methylcyclohexane, Propylcyclohexane, Isobutene, 1-Butene, Trans-Butene, Cis-Butene, Benzene, Propyne, Methanol, Ethanol, Toluene, Acetone, Dimethylether 13 HFC R125, R143a, R32, R1234yf, R134a, R227ea, R161, R1234ze, R152a, R236fa, R236ea, R245fa, R365mfc 3 FC R218, Perfluorobutane (C4F10), RC318 8 Siloxanes MM, Mdm, Md2 m, Md3 m, Md4 m, D4, D5, D6 2 Other Ammonia, water				ΔTmin)con=3 ΔTmin)ev =5 °C	0.92 and a supercritical cycle with a reduced pressure between 1.1 and 1.6. Among fluids with a similar critical temperature, fluids with high molecular complexity are preferable because of the possibility to reduce the average temperature differences in the primary heat exchanger, hence limiting the exergy losses.	have a saturated cycle configuration. RC318, C4F10 and R227ea appear as the best fluids from the thermodynamic point of view.
13	Ng, et al. [65]	(5)[a]cyclopentane, heptane, octane, methanol and ethanol	353–392 Cooling water 89^{0}C	WHR Diesel engine (marine)	η_{th}, η_{ex} based on the operating profile and machinery design data	Simple, recuperated, dual heat source, and with intermediate heating. ηt= 0.80, ηp = 0.80	Highest Pn and η_{th} for recuperative and simple with dual heat source ORC. The higher value of η_{th} was about 20 % Cyclopentane,18 % 15.2 %, for methanol and ethanol respectively.	Best WF is Cyclopentane, while the worst were for ethanol and methanol. η_{th}=cons with changing loads while Pn increased
14	Bekiloğlu HE et al. [66]	(28)[a] (HCs, HFCs and HFOs R1234yf,R1234ze (e),R1234zd(e), R134a, R152a,R143a R227ea,R236fa,R236ea, R245ca, R245fa,R32, R365mfc. Isohexane, Hexane, Heptane, Cyclohexane, Propylene, Benzene, Butane, Isobutane, Isopentane, Propane, Octane, Pentane Neopentane, Propyne,Toluene	90, 120 and 150 °C	Geothermal	Design an ORC with minimum UA per Pn and maximum performance factor (PF) with variables are specific speed, Pc, PR at the turbine stage, ΔT_{sup} and ΔT_{min} in the evaporator.	Simple with 1-D radial-inflow turbine.	Pn and η_{th}, UA turbine size increases with T_{hs} but rotational speed decreases. R227ea gives a lower UA value. Degrees of superheating of R134a and R152a have the highest values.	R1234yf, R1234ze(e) and isobutane are found to be the optimum working fluids at 90, 120 and 150 °C T_{hs} respectively And R134a is present in all ideal groups. However, when R134a is used, a higher degree of superheating is needed to avoid droplet formation in the turbine
15	Herath et al. [29]	(7)[a] R-134a, R-245fa, Benzene, Methanol, Ethanol, Acetone and Propane	100–200 ^{0}C	WHR	η_{th}, work ratio, the specific mass flowrate	Simple. ηt= 0.80, ηp = 0.70	η_{th} increases when increasing the Tev and Pev. and by decreasing the Pcon and Tcon. When the condenser temperature increases, the amount of fluid required to produce a unit power output also increases.	Benzene and Methanol based ORC systems perform more efficiently. The R-134a and R-290 (Propane) need higher operating pressures Moreover, it can be seen that Benzene, Methanol and Ethanol perform at high efficiencies at high temperatures

(*continued on next page*)

Table 4 (*continued*)

No	Reference	Type of WFs	T_{hs} (°C)	Heat resource	Objective of study	Cycle type and significant parameters	Main results	Notes
16	Toffolo et al. [67]	isobutane and R134a	130 and 180 °C	Geothermal	Maximizing the power output might be preferred for technical and economic reasons.	Subcritical and supercritical ORC systems. η_t= 0.85, η_p = 0.70	The maximum power output of R134a is higher than isobutane	Optimal cycle configuration is subcritical for isobutane and supercritical recuperated for R134a
17	Imran et al. [68]	(6)[a] R245fa, R600, R600a, SES36, R601a, and R601	160^{0}C	WHR	minimum specific investment cost and maximum exergy efficiency under logical bounds of evaporation temperature, pinch point temperature difference and superheat.	Simple ORC, recuperated ORC, and regenerative ORC system η_t= 0.75, η_p = 0.60 $\Delta Tmin)_{con}$= $\Delta Tmin)_{ev}$ =8 °C	For low temperatures, R134a, for mid-range temperatures, R245fa, and temperature of heat source, OMTS, pentane, and toluene are preferred. Basic ORC system has the lowest exergy efficiency, thermal efficiency, and specific investment cost but highest net power. The regenerative ORC system has the highest exergy efficiency and the specific investment cost. But the net power of the regenerative ORC system is lower than the basic ORC	Working fluids with critical temperatures in the same range of heat sources results in better thermal performance. R245fa has the highest Exergy efficiency of 51.3 %, corresponding to a minimum specific cost of 2423$/kW for the basic cycle, 53.74 %, corresponding to 2475$/kW for recuperated, and 55.93 %, corresponding to 2567$/kW for the regenerative cycle.
18	Kolasinski, [69]	(20)[a] R113,R114, R123, R124, R1234ze,R134a, R152a,R227ea,R236fa, R365mfc,R245ca, R245fa,R601a,R141b, R142,R236ea,R600a, RC318, R1234yf,R290	40–150^{0}C	WHR	η_{th},Pn with PR, WER, and volumetric expansion machines	Simple with volumetric expanders ηt= 0.7	With T_{hs} the Pn and η_{th} increased . For each WR there is max PR gives higher Pn. There is best value of η_{th} depending on WF and PR for each fluid.	The best WF are R123, R290, R600a,134a for different types of volumetric expanders. The PR for screw expander (10–15), for scroll (2–4.5) and the max pressure doesn't exceed 1.5 MPa
19	Shengjun et al. [70]	(16)[a]R123, R245ca, R245fa, R600, R600a, R236ea, R236fa,R227ea, R134a, R143a, R152a, R218, R125,R41,R170, CO_2	90^{0}C	Geothermal	. η_{th}, η_{ex}, LEC, recovery efficiency and heat exchanger area per unit power output (APR)	Simple, transcritical Subcritical. η_t=0.8, η_p = 0.75, ΔTmin)con= ΔTmin)ev =5 °C	Fluids favored by the η_{th} and η_{ex} are R123, R600, R245fa, R245ca and R600a. High recovery efficiency is obtained for R218, R125 and R41. Low APR value is presented for R152a, R134a, R600 and R143a. Low LEC value is observed for R152a, R600, R600a, R134a, R143a, R125 as well as R41. The best WF was R125 and R123 for transcritical and subcritical cycles, respectively	The optimum operation parameters are not the same for different indicators. The transcritical power cycle with R125 as the working fluid was a cost-effective lower than that of R123 in subcritical ORC. Reducing more CO2 emission. However, the APR of R123 was 40 % larger than that of R152a, leading to the highest APR value.

(continued on next page)

Table 4 (*continued*)

No	Reference	Type of WFs	T_{hs} (°C)	Heat resource	Objective of study	Cycle type and significant parameters	Main results	Notes
20	Ge, Zhong et al. [71]	(8)[a]Cyclopentane, cyclohexane, benzene, toluene.R1234ze(E), R600a, R245fa, R601a	250–350^{0}C	WHR (ICE)	Relation between Tev,Tcon, (ΔT)sup and Pn, η_{th}, exergy destruction rate	ORC with high-temperature loop (HTL) and low-temperature loop (LTL) η_t=0.8, η_p = 0.75, ΔTmin)con=5 ΔTmin)ev =10–20 °C,	The optimal Pn for T_{ev} (250–325 °C), HTL and Cyclopentane as WF.For 330–350 °C,cyclohexane. When Tev is above 350 °C, benzene is the optimal HTL working fluid for the R1234ze (E) for LTL	The superheat cycle can improve the net power output for the cyclopentane system with *Tev* of 295–325 °C. Variations in the exergy destruction rates related for WFs with *Tev* are distinct for the different HTL
21	Korolija and Greenough, [72]	(10)[a] 3cyclic siloxanes (D4, D5 and D6) and 4 linear siloxanes (MDM, MD2 M, MD3 M and MD4 M);3 aromatic fluids (Toluene, o-Xylene and p-Xylene)	465 °C to 350 °C	Foundry waste heat.	Influences local climate on the performance of the (ORC). η_{th} and the annual performance of the system	Simple and with IHE using air and water cooled condenser. . η_t=0.8, η_p = 0.60, ΔTmin)con= ΔTmin)ev =10 °C, ε=0.8	The IHE improve η_{th} from 17 to 25 % Increase T_a lead to improve η_{th} . The degree of improvement reduces with increasing outdoor air temperature.	Water cooled condenser effected more than air cooled. The best WF were Toluene, MDM and D4
22	Barse et al. [73]	(12)[a] R601, R601a, R123, R245ca, R245fa, R600, R600a, R236fa. R152a, R227ea, R134a, R236ea	100^{0}C	Geothermal	η_{th}, η_{ex},Pn and LCOE using a non-constrained and constrained design.	Simple ORC. η_t= η_p = 0.80, ΔTmin)con= ΔTmin)ev =6 °C	There is a strong correlation between the working fluid's critical temperature and the working fluids' efficiency. Based on the overall cost analysis, R245ca, R601a, R601, R245fa and R236ea show better performance among the 12 selected fluids in non-constrained design.	Optimizing the system design can increase η_{th} as high as 25 % in the case of R600. On the other hand, R227ea and R134a did not show significant increases in thermal efficiency. The decrease in LCOE can be as low as 11 % for R245ca by using a non-constrained design. For R600a, R152a, and R227ea, the LCOE was similar for the constrained design as compared to the optimized design.
23	Hung el.at. [52]	(11)[a] R–11, R–12, R–113, R–114, R–123, R–152a, R–500, and R–502; C6H6, C7H8, and C8H10	40 to 60 °C	Solar +otec	$\eta_{th.}$ Pn	Simple and combination solar+otec	$\eta_{th,}$ Pn increases nearly linearly as the Tint increases from 40 to 60 °C and T_{con} decreased from 20 to 5 °Cfor all WFs.	For lowest turbine inlet temperature, dry fluids refrigerant and benzene-series have almost the same. As the turbine inlet temperature increases, benzene group have higher η_{th}
24	Wang H et al. [74]	HFE7000, HFE7100 and HFE7500	150^{0}C	WHR	Effect of Tint of expander on Pn η_{th} and turbine size factor	Simple ORC, dry fluids without superheating . η_t= η_p = 0.80, $ΔTmin)_{con}$= $ΔTmin)_{ev}$ =5 °C	.η_{ex} η_{th} increase with the Tint but the slope of the curves decreases. The turbine size factor always decreases as the Tint increases.	There is optimum Tint lead to Pn max for all fluids but the best one HFE7000 which has the lowest boiling temperature.
25	Deethayat et al. [75]	R245fa/R152a zeotropic refrigerant with various compositions	115^{0}C	WHR	Effects of T_{ev}, mass fraction of R152a and ε of IHE on the ORC for η_{th},η_{ex}	(ORC) with internal heat exchanger (IHE). saturated condition. η_t= 0.85, η_p = 0.80, ε=0.8 $ΔTmin)_{con}$= 3, $ΔTmin)_{ev}$ =6 °C	Reduction of R245fa composition could reduce the irreversibilities at	of R245fa was around 80 % mass fraction and below. Higher effectiveness and evaporation

(*continued on next page*)

Table 4 (*continued*)

No	Reference	Type of WFs	T_{hs} (°C)	Heat resource	Objective of study	Cycle type and significant parameters	Main results	Notes
							the evaporator and the condenser	temperature resulted in higher efficiency.
26	Pierobon et al. [76]	(22)[a]R1234YF, R1234ZE,hexane, i-hexane, heptane, decane, nonane, octane, dodecane, methylcyclohexane, propylcyclohexane, cyclohexane, cyclopentane and cyclopropane, acetone, ammonia, benzene, ethanol, methanol, carbon dioxide, toluene and trifluoroiodomethane.	375 °C	WHR from gas turbine	Optimaision η_{th}, the total volume of the system and net present value. Variables are the working fluid, the turbine inlet pressure and temperature, the T_{con}, the pinch points and the fluid velocities in the heat exchangers.	Simple ORC with five different heat exchangers. η_t= 0.80, η_p = 0.80 ΔTmin)con= 10–25, ΔTmin)ev =10–30 °C	Cyclopentane and acetone, as optimal. Cyclopentane generally shows the highest efficiency but at the cost of greater total volumes and investment. However, regarding the net present value, Cyclopentane is the best choice.	Other promising working fluids are cyclohexane and hexane .
27	Uusitalo, et al. [13]	(35)[a]Three groups 0.8 Siloxanes, as D4, MD2 M, MDM, and MM; 20 (HCs) as toluene, isopentane, octane, cyclohexane, decane, pentane and butane and 7 fluorocarbons(HFCs) as R227ea,R134a, R245fa, and R365mfc. .	300 °C	WHR	Impact of molar mass and T_{cr} on $\eta_{th,}$ expansion ratio ER and condensing pressure P_{con}	ORC with reheating, superheating =10 °C, p_{ev-max}/p_{cr}=0.9, T_{con}=50 °C	WF with the higher T_{cr}, the higher η_{th} the lower condensing temperature and higher expansion ratio. High η_{th} can be obtained with high T_{cr} high T_{in} and high molar mass fluids gives high $\eta_{th.}$ .Siloxanes and HCs have higher η_{th} than for HFCs	Siloxanes and high critical temperature hydrocarbons represents low $P_{con.}$ Siloxanes D4 and D5 provide good thermal efficiencies but require larger turbine sizes and lower condenser pressures.
28	Abbas, et al. [77]	Butane, pentane, cyclopentane (MM)	80–280°C	WHR	Effect of heat source temperature T_{hs}, turbine inlet pressure Pev, PR, and ΔT_{sup} on η_{th}, η_{ex}	High-temperature cycle (HT-ORC) and the low-temperature cycle (LT-ORC	With an increasing T_{hs},PR,P_{ev},T_{cr} and superheating degree the thermal efficiency raised for all working fluids, from 3.3 % to 8.0 % for MM and from 1.9 % to 5.4 % for butane.	The η_{th}, η_{ex} increases when the P_{ev} rises. The η_{th} increases slightly with the ΔT_{sup} to a maximum and then decreases slightly for all working fluids, with the best value ΔT_{sup} being between 3 and 6 °C.
29	Wang. et al. [78]	(14)[a] (R113, R141b, R11, R123, R21 R245fa, R114, isopentane, butane, R236ea, R142b, Isobutene, R236fa, R124	150 °C	Geothermal water	Comprehensive performance (thermodynamic and economic) on 3 different configurations of ORC	Three ORCs (basic, regenerative and extractive ORCs)	The R141b shows the best comprehensive performance for basic ORC. The basic ORC performs the best among these 3 ORCs in terms of comprehensive thermodynamic and economic performances when using R245fa	The optimal η_{th} of simple ORC when employed to each of the 14 fluids increases with respect to the increase of their critical temperature
30	Li, P., et al. [79]	(5)[a] R245fa, R114, R245ca, R236ea and R365mfc	(125–160)° C		Effect of variable turbine efficiency on (ORC)	Simple ORC. The water at ambient temperature (293.15 K). The isentropic efficiency for the cycle pump is 0.7. the T_{ev} varies from 363.15 K to 393.15 K,	Increase T_{hs}, the PER, $\eta_{tur,}$ and η_{ex} decreased, while the η_{tur} for R365mfr higher than for 245fa. The net power output for different working fluids varies significantly	Raising T_{ev} from 90 to 110, the Pn, friction loss coefficient, leakage loss coefficient increased too, but the turbine efficiency declined

non-dimensional numbers like Carnot cycle efficiency and Jaacob number are critical in selecting appropriate WF for subcritical and supercritical cycles.

6.1. Condensing pressure (Pcon)

Lowering the P_{con} generally increases P_n, η_{th}, and sizing parameter (SP) [29]. This is due to the increased specific volume and enthalpy difference at the expander outlet. However, optimal P_{con} should remain within practical limits for WFs. The optimal condensing pressure ranges from 10 to 500 kPa for fluids like R113, R123, R141b, MM, ethylbenzene, etc. Some WFs exhibit very low condensing pressures (e.g., D5, MD2 M, Decane, Nonane) while others exceed 1000 kPa (e.g., R142b, R124, R227ea) [59]. The best candidates for efficient performance and practical P_{con} include cyclopentane, hexane, and benzene.

6.2. Condenser temperature (T_{con})

An increase in T_{con} reduces η_{th}, η_{ex} and P_n while increasing APR and η_{tur} [11,29,68,79,89], The pinch point temperature difference (ΔT_{min}) in the condenser also increases with T_{con}, reducing the Ac, although P_n has a more pronounced impact on APR than A_c. The proximity between condenser and ambient temperatures significantly impacts system irreversibility and efficiency. The optimal temperature difference is around 5–15 °C [22]. Lower ambient temperatures increase P_n and η_{th}, especially in simple cycles [90]. For specific fluids, the thermal efficiency improves by 16 % for MDM with water cooling and 8 % for air-cooled condensers. The increasing impact of the temperature difference between T_{db} and T_{wb} significantly affects heat transfer in the condenser. This temperature difference influences the cooling effectiveness and overall system performance, particularly in regions with varying humidity levels, further impacting η_{th} and P_n[60].

6.3. Evaporation pressure (P_{ev})

The effect of P_{ev} on P_n was analyzed using forty-two (42) dry, isentropic pure working fluids in subcritical cycles. Results showed that increasing P_{ev} raised P_n and η_{th}. However, higher pressure led to decreased P_n for certain hydrocarbons (e.g., Xylene group, Nonane, Decane, Ethylbenzene). Recommended working fluids included R113, R141b, Cyclohexane, Cyclopentane, Benzene, and Toluene [59]. Feng et al. [60] noted that for R123, as P_{ev} increased, η_{th} and η_{ex} also rose, while the APR decreased initially before rising again, and P_n showed the opposite trend. This behavior resulted from the ΔH in the expander and decreasing mass flow rate (m wf), leading to lower P_n at higher P_{ev}. Herath et al. [29], confirmed that benzene was optimal up to 4 MPa and 100–200 °C. R-134a and R-290 (Propane) required higher operating pressures, while Benzene, Methanol, and Ethanol performed well at elevated temperatures. Vélez et al., [90] found that increasing the pressure ratio (P4/P5) up to 5 for R134a, with T_{hs} around 150 °C, significantly improved efficiency. Moreover, adding an internal heat exchanger increased maximum efficiencies to 11 % for the basic cycle and 14 % for the modified cycle. Tchanche et al., [22] concluded that the η_{th} rises with p_{int}, reducing overall irreversibility.

6.4. Evaporation temperature (T_{ev})

Numerous studies have examined the relationship between T_{ev} and thermodynamic performance in various configurations of ORCs [11,22,29,58,60,70,71,75,77,82,90]. The trends observed for T_{ev} are similar to those for P_{ev} [60,77]. Increasing the T_{int} raises the V_5 and affects η_{th} and η_{ex}, which have optimal values for each fluid based on PR. For economic reasons, fluids with lower volume flow rates are preferred [22]. T_{ev} is crucial for optimizing low- and medium-temperature cycle performance [38]. According to Igbong et al. [58]., as T_{ev} increases to 160 °C, P_n, η_{th} (R601a=17 %), η_{ex}(R236fa =65 %) increases for all fluids, except for R601a and R365mfc, where the P_n decrease with T_{ev} higher than 120 °C. For low T_{ev} (60–84 °C), R134a, the η_{th} improved from 7 % to 9 % [11]. Also, Shengjun et al., [70] confirm that higher T_{ev} enhances η_{th}, η_{ex}, with R125 exhibiting the highest η_{th} (20 %) and recovery efficiency among 12 fluids investigated, while R123 reached η_{th} (11.1 %) in subcritical cycles. For high T_{ev} (200–300 °C), Algieri and Morrone [82], reported that increasing T_{ev} improved thermal efficiency and P_n for toluene, cyclohexane, and decane. The simple saturated cycle with toluene yielded the best efficiency, followed by transcritical with decane and superheated with cyclohexane. The introduction of IHE showed that the transcritical cycle with decane outperformed other configurations. These findings highlight that the impact of T_{ev} varies with the cycle's configuration and fluid used [82]. Additionally, Ge et al. [71] identified optimal P_n for T_{ev} (250–325 °C) for HTL, Cyclopentane, and cyclohexane for 330–350 °C. Beyond 350 °C, benzene was optimal for HTL, while R1234ze (E) was ideal for LTL. Wang et al., [78]noted that increasing T_{int} raises the thermodynamic efficiencies for HFE7000, HFE7100 and HFE7500, decreasing the turbine size factors and peak net power output, with HFE7000 being the best choice for converting low-grade heat to power. Higher ε and T_{ev} of zeotropic WFs also enhanced η_{th} and η_{ex}, as reported by Deethayat et al. [75].

6.5. Degrees of superheat (ΔT_{sup})

Increasing the ΔT_{sup} decreases P_n, while η_{th} and the APR increase. The η_{ex} shows minimal variation with ΔT_{sup} [60]. According to Hung et al. [52], for dry WFs, η_{th} decreases with higher superheat, where it increases for wet fluids. As ΔT_{sup} increases, the expander size increases, but m_{wf} decreases more rapidly than the enthalpy difference(ΔH) in the expander, resulting in P_n. Consequently, η_{th} rises while η_{ex} remains relatively constant. The increase of ΔT_{sup} also allows for a large A_{tot}, which increases faster than P_n, thus enhancing the APR. Imran et al. [65] noted that higher superheat slightly increases exergy efficiency and SIC. Additionally, greater degrees of superheat enable a more significant enthalpy difference in the expander while reducing the mass flow rate. However, as the superheat rises, exergy destruction in the evaporator decreases.

6.6. Pinch point temperature difference ($(\Delta T_{min})_{ev}$)

As the pinch point temperature difference $(\Delta T_{min})_{ev}$ increases, the P_n and η_{ex} decrease while the APR increases. However, the η_{th} remains relatively constant. [60]. The decrease in P_n is attributed to reductions in m_{wf} and ΔH in the expander. Consequently, η_{ex} declines due to lower m_{wf} and P_n. At the same time, an increase in $\mathbf{(\Delta T_{min})_{ev}}$ results in a decrease in A, which declines faster than P_n, thus enhancing the APR. Imran.el.at [68] noted that $\mathbf{(\Delta T_{min})_{ev}}$ positively affects the economic performance of the system, identifying an optimal pinch point for each cycle and WF. Specifically, at an optimum pinch point temperature difference of 7.5 °C, the basic ORC system achieves a minimum specific investment cost of 2245 $/kW and a maximum exergy efficiency of 42.81 %. In comparison, the recuperated ORC system has a minimum cost of $2390/kW with an exergy efficiency of 46.84 %, and the regenerative ORC system has a minimum cost of $2561/kW with a maximum efficiency of 52.25 %. Choosing ΔT_{min} depends on the types of WFs on both sides of the heat exchangers. For liquids, ΔT_{min} typically ranges from 5 to 20 °C [48,91], while for gaseous fluids, it is around 30 °C [23,57], due to differing heat transfer rates. Higher ΔT_{min} values can result in larger heat losses, whereas lower temperature pinches may increase the overall heat transfer area (UA) and system costs. Each system thus has an optimal ΔT_{min}. As concluded by Zhang et al. [62]., the optimal $(\Delta T_{min})_{ev}$, shows a decreasing trend with the rising critical temperature of WFs at specific heat source temperatures. Practically, $(\Delta T_{min})_{con}$ is usually around 5 °C, while general $(\Delta T_{min})_{ev}$ is around 20 °C. Other factors, including the acid dew point, chemical composition of the medium, and variations in ambient conditions, should also be considered.

6.7. Regeneration or preheating

Preheating does not directly affect power output, but its impact on efficiency depends on the working fluid. For instance, with an effectiveness of 0.8, the efficiency for R113 improves from 10.0 % to 13.8 %, and for R141b, it increases from 12 % to 12.6 % [59]. Various optimization methods, such as improving η_{ex}, η_{th}, P_n, and APR, can be applied to regenerative ORCs [60]. Altun et al. [11]. found that incorporating an internal heat recovery system increased the η_{th} and η_{ex} of the AFJET geothermal power plant by 15 %. Similarly, Algieri and Morrone [82] and Imran et al. [68] concluded that including IHE also improves the η_t and P_n, although the effect varies across working fluids. Deethayat et al. [75]. demonstrated that using an IHE with zeotropic WF R245fa/R152a enhanced η_{th}, η_{ex}, while reducing irreversibility in the evaporator and condenser.

6.8. Critical pressure and temperature (P_{cr}, T_{cr})

The critical parameters (P_{cr}, T_{cr}) are key in selecting WFs and organizing ORC operations. If the critical temperature T_c is below T_a, condensation and pumping cannot occur, disrupting the cycle's basic operation. Fluids with high P_{cr} allow the use of high P_{ev}, while those with high T_{cr} enable the use of high-temperature heat sources. Hærvig, et al. [92] suggest that for maximum P_n, the optimal T_{cr} for pure fluids is 30–50 °C above T_{hs}, while for mixtures, it should be 30–50 °C below T_{hs}. Fluids with lower critical temperatures generate less P_n, but this trend reverses for thermal efficiency, which improves with temperature [73]. Low critical pressures and temperatures are advantageous in supercritical ORC systems. He et al., [55] fluids with T_{cr} close to the heat source temperature produced higher P_n, though excessively high T_{cr} (>230 °C) negatively affects P_n. Some fluids, like octane and toluene, with higher T_{cr}, face condensation issues, resulting in lower power output [63]. Hydrocarbons with higher T_{cr} increase thermal efficiency but lower volumetric work output, requiring a balance between critical points for optimal performance [93]. Tang et al., [19] found that fluids with T_{cr} close to optimal values (T_{cropt}) enhance heat transfer and efficiency, with differences (T_{hs}-T_{cropt}) not exceeding 30 °C. Higher T_{cr} fluids benefit most in non-constrained designs, reducing levelized electricity costs (LCOE) compared to constrained designs, whereas low T_{cr} fluids show minimal improvement [73]. Igbong et al. [58] confirmed that higher T_{cr} fluids have higher specific power (SP) and volumetric flow rate (VFR), although fluids with lower SP and VFR are preferable for efficiency.

6.9. Heat source temperature (T_{hs})

T_{hs} and the pinch point $(\Delta T_{min})_{ev}$ are crucial in determining the T_{ev} and maximum P_{ev} of the ORC. As T_{hs} increases, P_n and η_{th} rise due to a larger enthalpy drop through the turbine. However, this effect varies based on the WF and cycle parameters [48,64,66,69,77]. For example, R365mfc shows a nearly linear increase in T_{ev} with T_{hs} (125–160 °C), while R245fa's increase slows at higher T_{hs}[79]. Lecompte et al., [53] It is important to consider heat profile variations during typical batch processes, such as those in electric arc furnaces. He et al., [55], found that the best results occur with WFs whose critical temperatures are 10–40 °C below the inlet T_{hs}, yielding higher P_n. For a T_{hs} of 150 °C, R114 and isobutane perform best, while R236ea and isobutane excel at 145 °C [17]. Siloxanes, especially MM and MDM, are noted for their excellent efficiency at high T_{hs} [81], with higher T_{cr} yielding better performance. T_{hs} also affects the volumetric expansion ratio (VFR) and the cycle type. For a T_{hs} of 200 °C, a single-stage system using a turbine produces the highest power. However, at higher T_{hs} (up to 300 °C), cascaded cycles outperform single-stage systems, producing up to 6 % more power due to reduced VFR in each cycle. The higher molar mass, like siloxanes, tends to have smaller P_{cr} and higher T_{cr}. However, no clear correlation exists between molar mass and critical temperature for fluorocarbons. Fluids with higher T_{cr} exhibit better thermal efficiency, lower condensing temperatures, and higher expansion ratios than other fluids in the same group. Siloxanes and hydrocarbons with high T_{cr} typically have very low condensing pressures, often below 0.1 MPa, especially at low condensing temperatures (50 °C), necessitating the use of multistage turbines, whether axial or radial [15]. T_{hs} also affects the VFR and the cycle type. For a T_{hs} of 200 °C, a single-stage system using a turbine produces the highest power. However, at higher T_{hs} (up to 300 °C), cascaded cycles outperform single-stage systems, producing up to 6 % more power due to reduced VFR in each cycle[87].

6.10. Isentropic efficiency of the turbine (η_t) and pump (η_p)

It was noticed during the analysis of previous studies that fixed values are imposed on η_t (0.75–0.85) and η_p (0.5–0.8), as summarized in Table 4, which leads to inaccurate results. The η_t of the turbine measures how effectively the turbine converts the available energy [64]. A higher turbine isentropic efficiency means more energy is converted, resulting in improved overall cycle performance. A lower efficiency, on the other hand, leads to energy losses and decreased cycle performance. A higher η_p means less work is required to achieve the desired pressure, resulting in reduced energy consumption and improved cycle performance. Conversely, a lower pump efficiency leads to higher energy consumption and decreased cycle performance. It should be noted that the effect of the η_t is much greater than that of the η_p on the performance characteristics of ORC. Enhancing η_t by 1 % improves the η_{th} by 2–3 %, depending on initial values of η_{th}. These efficiencies directly affect the power output, thermal efficiency, and specific work output of the ORC system. Therefore, it is crucial to design and select turbines and pumps with high isentropic efficiencies to maximize the performance and efficiency of the ORC. It's worth noting that various factors, including the components' design, size, and operating conditions, can influence the isentropic efficiency of the turbine and pump. Proper selection, sizing, and optimization of the turbine and pump based on the specific requirements of the ORC system are essential to achieve the desired performance levels. It should be noted that it is not necessary for the optimal values of the thermodynamic parameters to be identical to the economic factors, so a compromise must be found. The results of previous research analysis indicate that no WF fulfills all the required specifications. Mixing more than one fluid may give better results, even though a group of WFs exists.

7. Conclusion

1. **Key Parameters Influence:** The most influential parameter on the cycle's performance is the temperature ratio (T_{ev}/T_{con}), followed by the pressure ratio (P_{ev}/P_{con}), latent heat, and specific heat. The results show that P_n increases with rising T_{ev}/T_{con} and P_{ev}/P_{con} ratios for most working fluids as the T_{hs} increases. However, the relationship between T_{cr}, T_{ev}, and P_n follows a parabolic trend. Working fluids with higher temperature ratios consistently enhance P_n and η_{th}. Low T_{cr} fluids tend to underperform in high-temperature applications, while high T_{cr} hydrocarbons and siloxanes excel in such conditions. On the other hand, HFCs and low T_{cr} hydrocarbons are better suited for low-temperature applications.
2. **Cycle Efficiency vs. Power Output:** The temperature (T_{ev}/T_{con}) and pressure (P_{ev}/P_{con}) ratios yield maximum η_{th} or η_{ex} often differ from those that maximize P_n. This variation depends on the working fluid and cycle configuration, requiring careful balancing of parameters based on the desired outcome.
3. **Performance of Siloxanes:** Simple linear siloxanes (MM, D4, MDM), which have higher molar masses, smaller P_{cr}, and higher T_{cr}, exhibit superior thermal efficiency. These fluids also benefit from

lower condensing temperatures and higher expansion ratios, making them well-suited for high T_{hs} applications.

4. **Exergy Destruction in Components:** The evaporator is identified as the system's primary source of exergy destruction, followed by the condenser. Therefore, optimizing these components is critical to improving overall system performance.
5. **Cycle Configuration for Subcritical Applications:** Superheating is not beneficial in subcritical cycles, and the optimal configuration typically features a saturated cycle with dry working fluids. This avoids unnecessary energy losses and ensures better system efficiency.
6. **Optimal Heat Exchangers:** The most efficient heat exchangers are finned tube bundles with circular fins for evaporators and shell-and-tube heat exchangers for condensers. The pinch point temperature difference (ΔT_{min}) ranges between 5 and 20 °C for liquids and around 30 °C for gaseous fluids.
7. **Heat Source Temperature's Role in WF Selection:** The choice of Rankine cycle applications—and thus the class of working fluids—is primarily dictated by T_{hs}. This temperature determines the maximum allowable temperature and pressure, which influences the design, sizing of ORC components, and overall system performance.
8. **Optimum Evaporation Pressure for Each WF:** For every working fluid, there is an optimal P_{ev} that yields the highest P_n and the best η_{th}. Selecting the correct P_{ev} for each fluid is critical to maximizing system performance.

This study establishes a clear relationship between performance outcomes and different working fluids characteristics under varying heat source conditions, providing new insights into optimizing fluid selection for specific applications. Identifying the evaporator as the primary source of exergy destruction offers a targeted approach to enhancing ORC system efficiency. Additionally, the analysis of subcritical cycle configurations underscores the conditions under which saturated cycles outperform superheated cycles, contributing valuable knowledge to ORC design strategies.

The proposed selection criteria and insights into optimal working fluids can guide the development of high-performance ORC systems for applications such as low-temperature geothermal energy, industrial waste heat recovery, and solar thermal power. These results directly affect designing efficient and cost-effective ORC systems tailored to site-specific conditions and heat sources.

8. Recommendations

1. **Environmental and Safety Screening of Working Fluids:** The selection of working fluids should begin with a thorough screening process to ensure they comply with environmental regulations and safety standards. This is essential for the sustainable and safe operation of the ORC system.
2. **Optimal Critical Temperature to Heat Source Temperature Ratio:** For achieving optimal plant efficiencies, it is recommended to maintain the ratio of T_{cr} to T_{hs} between 0.88 and 0.92. The difference between the T_{hs} and $Tcr_{\text{-}opt}$ should ideally range between 10 and 40 °C and must not exceed 30 °C.
3. **Turbine Configuration for High T_{hs}:** Multistage turbines—either axial or radial—and cascaded expanders are preferable for systems with high Ths. High-critical temperature fluids with lower specific power (SP) and VFR are ideal. However, a single-stage turbine is recommended for systems with T_{hs} below 200 °C.
4. **Accounting for Variable Turbine Efficiency:** Fixed values for η_t were often assumed in past studies, which may lead to inaccuracies in performance estimation. It is therefore recommended that variations in efficiency be accounted for to achieve more precise results.
5. **Optimal Working Fluids for Different Heat Source Temperatures:** For T_{hs} up to 300 °C, working fluids such as Cyclopentane, Toluene, Hexane, and Pentane are ideal. For T_{hs} below 200 °C, fluids such as R600, R600a, R152a, Isobutene, R1233zd(E), R1234yf, and Cyclohexane are recommended. Benzene is a suitable choice for heat sources between 350 and 500 °C.
6. **Promising Potential of Binary Isothermal Mixtures:** Expanding research on binary isothermal mixtures is highly recommended, as these mixtures offer better energy efficiency than single-component or pure isothermal fluids. This advantage comes without superheating or regeneration, making them a promising future direction for ORC systems.

CRediT authorship contribution statement

Mohammad Shalby: Writing – review & editing, Writing – original draft, Supervision, Conceptualization. **Abdullah Marachli:** Writing – original draft, Supervision, Project administration, Formal analysis. **Ahmad A Salah:** Writing – review & editing, Validation, Resources, Conceptualization.

Declaration of competing interest

The authors declare that they have no known competing financial interests or personal relationships that could have appeared to influence the work reported in this paper.

Data availability

Data will be made available on request.

References

[1] S. Algarni, et al., Contribution of renewable energy sources to the environmental impacts and economic benefits for sustainable development, Sustainable Energy Technologies and Assessments 56 (2023) 103098.
[2] A.A. Salah, M.M. Shalby, F.Basim Ismail, The status and potential of renewable energy development in Jordan: exploring challenges and opportunities, Sustainability: Science, Practice and Policy 19 (1) (2023) 2212517.
[3] M. Sarfraz, M. Khan, Energy optimization of water-based hybrid nanomaterials over a wedge-shaped channel, Scientia Iranica 31 (1) (2024) 71–82.
[4] S.R. Salkuti, Modeling of various renewable energy resources for smart electrical power systems. Next Generation Smart Grids: Modeling, Control and Optimization, Springer, 2022, pp. 29–47.
[5] H. Jouhara, et al., Waste heat recovery technologies and applications, Thermal Science and Engineering Progress 6 (2018) 268–289.
[6] G.P. Varma, T. Srinivas, Power generation from low temperature heat recovery, Renewable and Sustainable Energy Reviews 75 (2017) 402–414.
[7] M.R. Gomaa, et al., A low-grade heat Organic Rankine Cycle driven by hybrid solar collectors and a waste heat recovery system, Energy Reports 6 (2020) 3425–3445.
[8] M. Villarini, et al., State of art of small scale solar powered ORC systems: a review of the different typologies and technology perspectives, Energy Procedia 45 (2014) 257–267.
[9] T. Mahlia, et al., Organic rankine cycle (ORC) system applications for solar energy: recent technological advances, Energies. (Basel) 12 (15) (2019) 2930.
[10] M.R. Gomaa, R.J. Mustafa, N. Al-Dmour, Solar thermochemical conversion of carbonaceous materials into syngas by Co-Gasification, J. Clean. Prod. 248 (2020) 119185.
[11] A.F. Altun, M. Kilic, Thermodynamic performance evaluation of a geothermal ORC power plant, Renew. Energy 148 (2020) 261–274.
[12] B.F. Tchanche, et al., Low-grade heat conversion into power using organic Rankine cycles–A review of various applications, Renewable and Sustainable Energy Reviews 15 (8) (2011) 3963–3979.
[13] P. Colonna, et al., Organic Rankine cycle power systems: from the concept to current technology, applications, and an outlook to the future, J. Eng. Gas. Turbine Power. 137 (10) (2015) 100801.
[14] R. Loni, et al., A review of industrial waste heat recovery system for power generation with Organic Rankine Cycle: recent challenges and future outlook, J. Clean. Prod. 287 (2021) 125070.
[15] A. Uusitalo, et al., Thermodynamic evaluation on the effect of working fluid type and fluids critical properties on design and performance of Organic Rankine Cycles, J. Clean. Prod. 188 (2018) 253–263.
[16] B.F. Tchanche, M. Pétrissans, G. Papadakis, Heat resources and organic Rankine cycle machines, Renewable and Sustainable Energy Reviews 39 (2014) 1185–1199.
[17] F. Vélez, et al., A technical, economical and market review of organic Rankine cycles for the conversion of low-grade heat for power generation, Renewable and Sustainable Energy Reviews 16 (6) (2012) 4175–4189.
[18] S. Carnot, Réflexions Sur La Puissance Motrice Du Feu, 26, Vrin, 1979.
[19] J. Tang, L. Kang, Y. Liu, An Effective Method for Working Fluid Design of Organic Rankine Cycle, Processes 10 (9) (2022) 1857.

[20] W. Fan, et al., Analysis of the thermodynamic performance of the organic Rankine cycle (ORC) based on the characteristic parameters of the working fluid and criterion for working fluid selection, Energy Convers. Manage 211 (2020) 112746.
[21] M. Imran, et al., Thermo-economic optimization of Regenerative Organic Rankine Cycle for waste heat recovery applications, Energy Convers. Manage 87 (2014) 107–118.
[22] B.F. Tchanche, et al., Fluid selection for a low-temperature solar organic Rankine cycle, Appl. Therm. Eng. 29 (11-12) (2009) 2468–2476.
[23] H. Zhai, et al., Categorization and analysis of heat sources for organic Rankine cycle systems, Renewable and Sustainable Energy Reviews 64 (2016) 790–805.
[24] T. Tartière, M. Astolfi, A world overview of the organic Rankine cycle market, Energy Procedia 129 (2017) 2–9.
[25] Bohl, R., Waste heat recovery from existing simple cycle gas turbine plants: a case study. 2009.
[26] X. Zhang, et al., Comparative study of waste heat steam SRC, ORC and S-ORC power generation systems in medium-low temperature, Appl. Therm. Eng. 106 (2016) 1427–1439.
[27] A.A. Naqvi, et al., An effective and simplified method to select the working fluid for waste heat recovery based Organic Rankine Cycle, Tecciencia (33) (2022) 17.
[28] D. Krempus, et al., On mixtures as working fluids of air-cooled ORC bottoming power plants of gas turbines, Appl. Therm. Eng. 236 (2024) 121730.
[29] H. Herath, et al., Working fluid selection of organic Rankine cycles, Energy Reports 6 (2020) 680–686.
[30] S. Eyerer, et al., Experimental investigation of modern ORC working fluids R1224yd (Z) and R1233zd (E) as replacements for R245fa, Appl. Energy 240 (2019) 946–963.
[31] G. Györke, et al., Novel classification of pure working fluids for Organic Rankine Cycle, Energy 145 (2018) 288–300.
[32] K. Thurairaja, et al., Working fluid selection and performance evaluation of ORC, Energy Procedia 156 (2019) 244–248.
[33] C. Carcasci, R. Ferraro, E. Miliotti, Thermodynamic analysis of an organic Rankine cycle for waste heat recovery from gas turbines, Energy 65 (2014) 91–100.
[34] S. Upadhyaya, V. Gumtapure, Thermodynamic analysis of organic Rankine cycle with Hydrofluoroethers as working fluids, in: IOP Conference Series: Materials Science and Engineering, IOP Publishing, 2018.
[35] A. Linde Gases, Refrigerants Environmental Data. Ozone Depletion and Global Warming Potential, Linde Gases AG Gases Division, Seitnerstrasse 70 (2019) 82049.
[36] J.A. Schwöbel, et al., High-throughput screening of working fluids for the organic Rankine cycle (ORC) based on conductor-like screening model for realistic solvation (COSMO-RS) and thermodynamic process simulations, Ind. Eng. Chem. Res. 56 (3) (2017) 788–798.
[37] G. Myhre, et al., Anthropogenic and natural radiative forcing, Climate Change 2013-The Physical Science Basis (2014) 659–740.
[38] M. Bahrami, F. Pourfayaz, A. Kasaeian, Low global warming potential (GWP) working fluids (WFs) for Organic Rankine Cycle (ORC) applications, Energy Reports 8 (2022) 2976–2988.
[39] C. Davenport, Nations, fighting powerful refrigerant that warms planet, reach landmark deal, New York Times (2016).
[40] J. Bao, et al., Comparative study of combined organic Rankine cycle and vapor compression cycle for refrigeration: single fluid or dual fluid? Sustainable Energy Technologies and Assessments 37 (2020) 100595.
[41] S. Lecompte, et al., Exergy analysis of zeotropic mixtures as working fluids in Organic Rankine Cycles, Energy Convers. Manage 85 (2014) 727–739.
[42] S. Douvartzides, I. Karmalis, in: Working fluid selection for the Organic Rankine Cycle (ORC) exhaust heat recovery of an internal combustion engine power plant. in IOP conference series: materials science and engineering, IOP Publishing, 2016.
[43] V. Kindra, et al., Thermodynamic Optimization of Low-Temperature Cycles for the Power Industry, Energies. (Basel) 15 (9) (2022) 2979.
[44] B.T. Liu, K.H. Chien, C.C. Wang, Effect of working fluids on organic Rankine cycle for waste heat recovery, Energy 29 (8) (2004) 1207–1217.
[45] X. Wang, et al., Working fluid selection for organic Rankine cycle power generation using hot produced supercritical CO2 from a geothermal reservoir, Appl. Therm. Eng. 149 (2019) 1287–1304.
[46] A.K. Bett, S. Jalilinasrabady, Exergoeconomic Analysis for Optimized Combined Wet and Dry Cooling BinaryPower Plant at Olkaria I, Kenya. Geothermics 95 (2021) 102160.
[47] A.F. Babatunde, O.O. Sunday, A review of working fluids for organic Rankine cycle (ORC) applications, in: IOP conference series: materials science and engineering, IOP Publishing, 2018.
[48] H. Zhai, L. Shi, Q. An, Influence of working fluid properties on system performance and screen evaluation indicators for geothermal ORC (organic Rankine cycle) system, Energy 74 (2014) 2–11.
[49] V. Chintala, S. Kumar, J.K. Pandey, A technical review on waste heat recovery from compression ignition engines using organic Rankine cycle, Renewable and Sustainable Energy Reviews 81 (2018) 493–509.
[50] S. Quoilin, et al., Working fluid selection and operating maps for Organic Rankine Cycle expansion machines, in: 21st international compressor conference at Purdue, 2012.
[51] S.S. Bajaj, et al., Organic Rankine Cycle and Its Working Fluid Selection—A Review, International Journal of Current Engineering and Technology 4 (4) (2016) 20–26.
[52] T. Hung, et al., A study of organic working fluids on system efficiency of an ORC using low-grade energy sources, Energy 35 (3) (2010) 1403–1411.
[53] S. Lecompte, et al., Case study of an organic Rankine cycle (ORC) for waste heat recovery from an electric arc furnace (EAF), Energies. (Basel) 10 (5) (2017) 649.
[54] M.E.M. Montagud, M. Thern, Non-conventional working fluids for thermal power generation: a review, Journal of Postdoctoral Research 2 (8) (2014) 1–14.
[55] C. He, et al., The optimal evaporation temperature and working fluids for subcritical organic Rankine cycle, Energy 38 (1) (2012) 136–143.
[56] C. Liu, et al., The optimal evaporation temperature of subcritical ORC based on second law efficiency for waste heat recovery, Entropy 14 (3) (2012) 491–504.
[57] I. Vaja, A. Gambarotta, Internal combustion engine (ICE) bottoming with organic Rankine cycles (ORCs), Energy 35 (2) (2010) 1084–1093.
[58] D. Igbong, et al., Working fluid selection for simple and recuperative organic rankine cycle operating under varying conditions: a comparative analysis. Advances in Science and Technology, Research Journal 15 (4) (2021) 202–221.
[59] S.L. Douvartzides, et al., Energy and Exergy-Based Screening of Various Refrigerants, Hydrocarbons and Siloxanes for the Optimization of Biomass Boiler–Organic Rankine Cycle (BB–ORC) Heat and Power Cogeneration Plants, Energies. (Basel) 15 (15) (2022) 5513.
[60] Y. Feng, et al., Sensitivity analysis and thermoeconomic comparison of ORCs (organic Rankine cycles) for low temperature waste heat recovery, Energy 82 (2015) 664–677.
[61] M. Bahrami, A.A. Hamidi, S. Porkhial, Investigation of the effect of organic working fluids on thermodynamic performance of combined cycle Stirling-ORC, International Journal of Energy and Environmental Engineering 4 (2013) 1–9.
[62] C. Zhang, et al., Thermo-economic comparison of subcritical organic Rankine cycle based on different heat exchanger configurations, Energy 123 (2017) 728–741.
[63] T. Zhang, et al., Correlation analysis based multi-parameter optimization of the organic Rankine cycle for medium-and high-temperature waste heat recovery, Appl. Therm. Eng. 188 (2021) 116626.
[64] M. Astolfi, et al., Binary ORC (Organic Rankine Cycles) power plants for the exploitation of medium–low temperature geothermal sources–Part B: techno-economic optimization, Energy 66 (2014) 435–446.
[65] C. Ng, I.C. Tam, D. Wu, Thermo-economic performance of an organic rankine cycle system recovering waste heat onboard an offshore service vessel, J. Mar. Sci. Eng. 8 (5) (2020) 351.
[66] H.E. Bekiloğlu, H. Bedir, G. Anlaş, Multi-objective optimization of ORC parameters and selection of working fluid using preliminary radial inflow turbine design, Energy Convers. Manage 183 (2019) 833–847.
[67] A. Toffolo, et al., A multi-criteria approach for the optimal selection of working fluid and design parameters in Organic Rankine Cycle systems, Appl. Energy 121 (2014) 219–232.
[68] M. Imran, et al., Comparative assessment of Organic Rankine Cycle integration for low temperature geothermal heat source applications, Energy 102 (2016) 473–490.
[69] P. Kolasiński, The method of the working fluid selection for organic Rankine cycle (ORC) systems employing volumetric expanders, Energies. (Basel) 13 (3) (2020) 573.
[70] Z. Shengjun, W. Huaixin, G. Tao, Performance comparison and parametric optimization of subcritical Organic Rankine Cycle (ORC) and transcritical power cycle system for low-temperature geothermal power generation, Appl. Energy 88 (8) (2011) 2740–2754.
[71] Z. Ge, et al., Thermodynamic performance analyses and optimization of dual-loop organic Rankine cycles for internal combustion engine waste heat recovery, Applied sciences 9 (4) (2019) 680.
[72] I. Korolija, R. Greenough, Modelling the Influence of Climate on the Performance of the Organic Rankine Cycle for Industrial Waste Heat Recovery, Energies. (Basel) 9 (5) (2016) 335.
[73] K.A. Barse, M.D. Mann, Maximizing ORC performance with optimal match of working fluid with system design, Appl. Therm. Eng. 100 (2016) 11–19.
[74] Y. Wang, et al., Multi-objective optimization and grey relational analysis on configurations of organic Rankine cycle, Appl. Therm. Eng. 114 (2017) 1355–1363.
[75] T. Deethayat, T. Kiatsiriroat, C. Thawonngamyingsakul, Performance analysis of an organic Rankine cycle with internal heat exchanger having zeotropic working fluid, Case Studies in Thermal Engineering 6 (2015) 155–161.
[76] L. Pierobon, et al., Multi-objective optimization of organic Rankine cycles for waste heat recovery: application in an offshore platform, Energy 58 (2013) 538–549.
[77] W.K.A. Abbas, E. Baumhögger, J. Vrabec, Experimental investigation of organic Rankine cycle performance using alkanes or hexamethyldisiloxane as a working fluid, Energy Conversion and Management: X 15 (2022) 100244.
[78] H. Wang, et al., Thermodynamic analysis of organic Rankine cycle with hydrofluoroethers as working fluids, Energy Procedia 105 (2017) 1889–1894.
[79] P. Li, et al., Multi-objective optimization and improved analysis of an organic Rankine cycle coupled with the dynamic turbine efficiency model, Appl. Therm. Eng. 150 (2019) 912–922.
[80] Y.A.A. Laouid, et al., Towards improvement of waste heat recovery systems: a multi-objective optimization of different organic Rankine cycle configurations, International Journal of Thermofluids 11 (2021) 100100.
[81] F. Fernández, M. Prieto, I. Suárez, Thermodynamic analysis of high-temperature regenerative organic Rankine cycles using siloxanes as working fluids, Energy 36 (8) (2011) 5239–5249.
[82] A. Algieri, P. Morrone, Comparative energetic analysis of high-temperature subcritical and transcritical Organic Rankine Cycle (ORC). A biomass application in the Sibari district, Appl. Therm. Eng. 36 (2012) 236–244.
[83] S. Quoilin, S. Declaye, V. Lemort, Expansion machine and fluid selection for the organic Rankine cycle, in: Proceedings of the 7th international conference on heat transfer, fluid mechanics and thermodynamics, 2010.

[84] M.E. Mondejar, M. Thern, Analysis of isentropic mixtures for their use as working fluids in organic Rankine cycles, Environ. Prog. Sustain. Energy 36 (3) (2017) 921–935.
[85] Tauveron, N. and D. Barbier, Low grade waste heat recovery in an intercooled recuperated closed cycle gas turbine. 2016.
[86] A. Biswas, B.K. Mandal, Analysis of Organic Rankine Cycle Using Various Working Fluids for Low-Grade Waste Heat Recovery, in: International Conference on Advances in Energy Research, Springer, 2022.
[87] M. White, M. Read, A. Sayma, Comparison between single and cascaded organic Rankine cycle systems accounting for the effects of expansion volume ratio on expander performance, in: IOP Conference Series: Materials Science and Engineering, IOP Publishing, 2019.
[88] D. Mikielewicz, J. Mikielewicz, Criteria for selection of working fluid in low-temperature ORC, Chemical and Process Engineering 37 (3) (2016).
[89] S.C. Yang, et al., Experimental investigation on a 3 kW organic Rankine cycle for low-grade waste heat under different operation parameters, Appl. Therm. Eng. 113 (2017) 756–764.
[90] F. Vélez, F. Chejne, A. Quijano, Thermodynamic analysis of R134a in an Organic Rankine Cycle for power generation from low temperature sources, Dyna 81 (185) (2014) 153–159.
[91] D. Maraver, et al., Systematic optimization of subcritical and transcritical organic Rankine cycles (ORCs) constrained by technical parameters in multiple applications, Appl. Energy 117 (2014) 11–29.
[92] J. Hærvig, K. Sørensen, T.J. Condra, Guidelines for optimal selection of working fluid for an organic Rankine cycle in relation to waste heat recovery, Energy 96 (2016) 592–602.
[93] R. Brignoli, J.S. Brown, Organic Rankine cycle model for well-described and not-so-well-described working fluids, Energy 86 (2015) 93–104.